PAUL SCHERRER INSTITUT

PSI

Wir schaffen Wissen – heute für morgen

Introduction to μSR practical
Scientific problem to be analyzed

Rustem Khasanov

Laboratory for Muon Spin Spectroscopy
Paul Scherrer Institut

PAUL SCHERRER INSTITUT

Outline

1. Scientific problems to be solved during the μSR practicum
   - Determination of the magnetic order parameter (ordered moment size) using ZF- μSR measurements in $BaFe_2As_2$
   - Determination of the magnetic penetration depth and obtaining gap(s) symmetry using TF- μSR measurements in $Ba_{0.65}Rb_{0.35}Fe_2As_2$
   - Measure the Meissner screening profile of a superconductor with Low Energy μSR in $YBa_2Cu_3O_{7-\delta}$
2. Muon experiments under the pressure
3. Pressure induced electronic phase separation in CrAs
   - Previous experiments
   - What μSR could do?
   - Ambient pressure data
   - Experiments under the pressure
4. Superfluid density and the symmetry of the superconducting gap
   - s-wave gap
   - d-wave gap
   - Multiple gaps

Muon practicum (exercises 1 and 2)

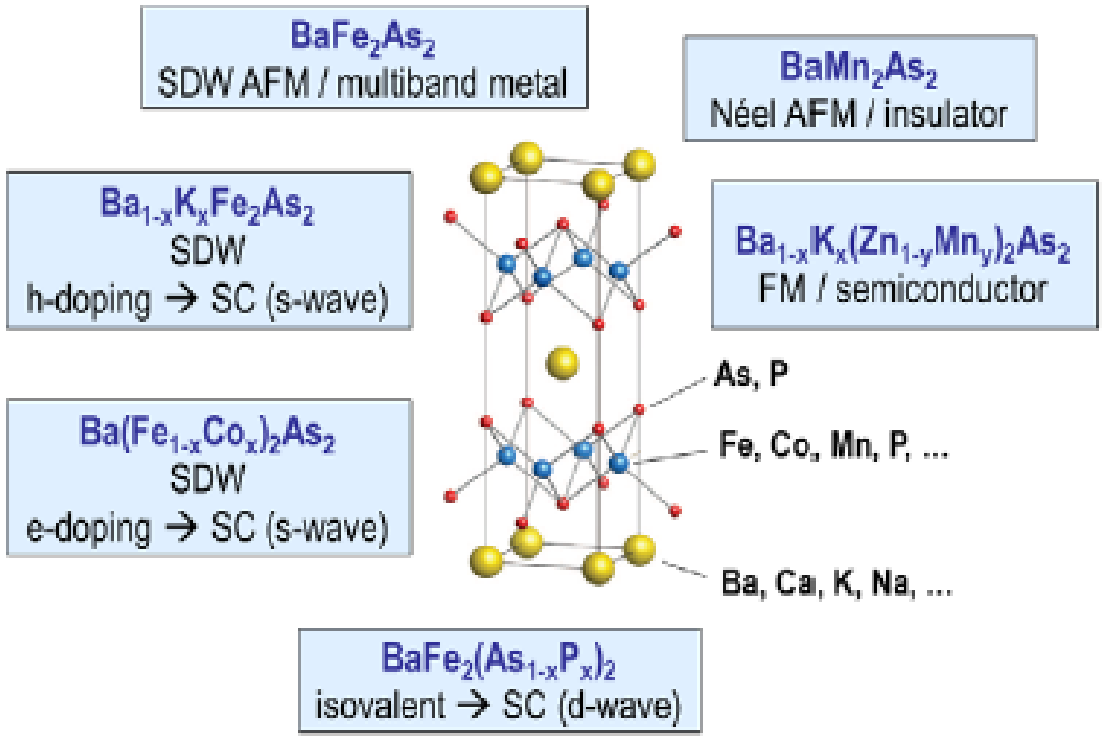

- *The structure is very flexible and a variety of interesting physical properties emerge by substitution with different elements*
- *The parent $BaFe_2As_2$ compound is antiferromagnet*
- *Doping by alakli metal (hole doping) cobalt (electron doping), isovalent substitution of As by P may lead to the occurrence of superconductivity.*
- *Substitution of Fe by Mn makes it insulating with antiferromagnetic structure*
- *Etc.*

PAUL SCHERRER INSTITUT

Exercise 1 ($BaFe_2As_2$)

Determination of the magnetic order parameter (ordered moment size) using ZF- μSR measurements.

Determination of the magnetic order parameter (ordered moment size) using ZF- μSR measurements.

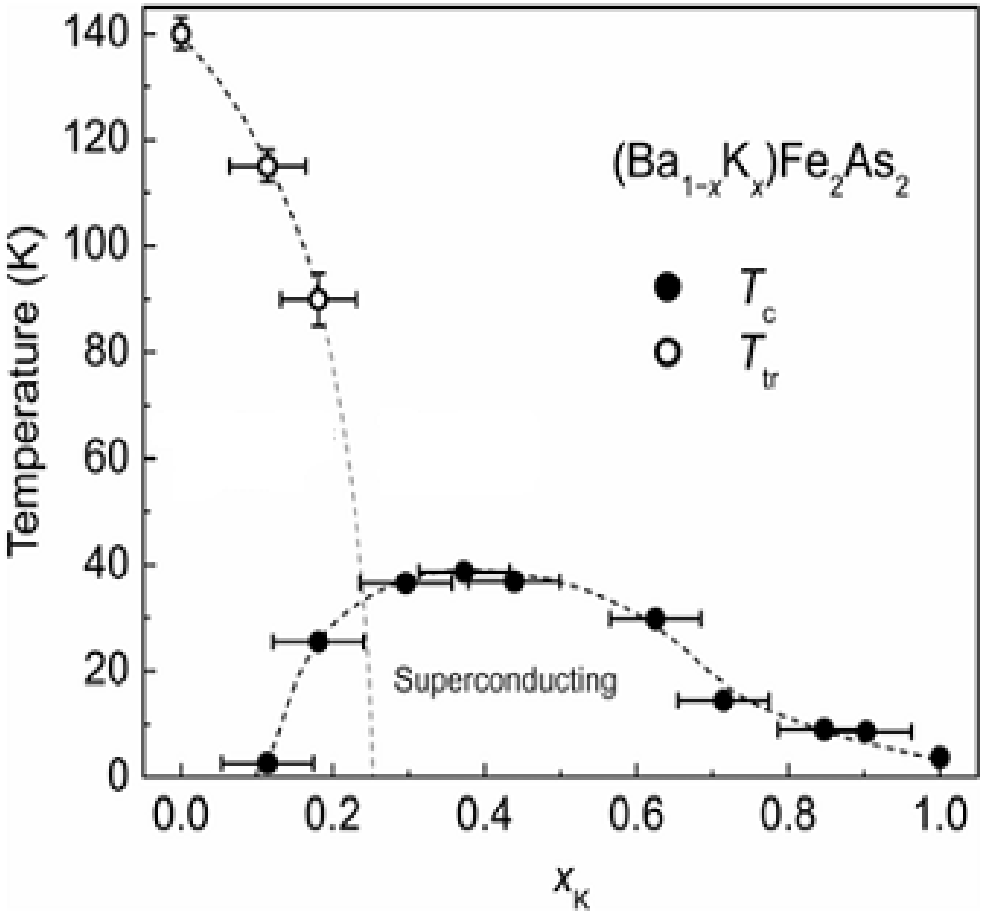

Obtain the internal field and follow its temperature evolution.

PAUL SCHERRER INSTITUT

Exercise 2 ($Ba_{0.65}Rb_{0.35}Fe_2As_2$)

Determination of the magnetic penetration depth and obtaining gap(s) symmetry using TF- μSR measurements.

Determination of the magnetic penetration depth and obtaining gap(s) symmetry using TF- μSR measurements.

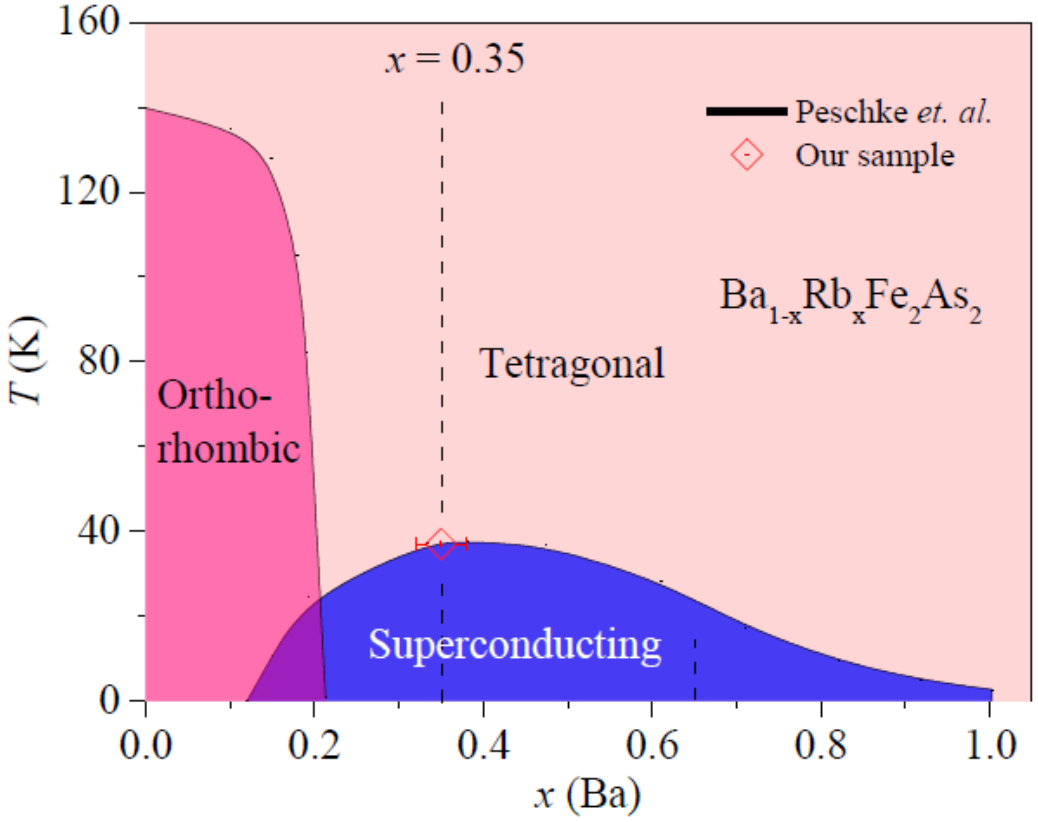

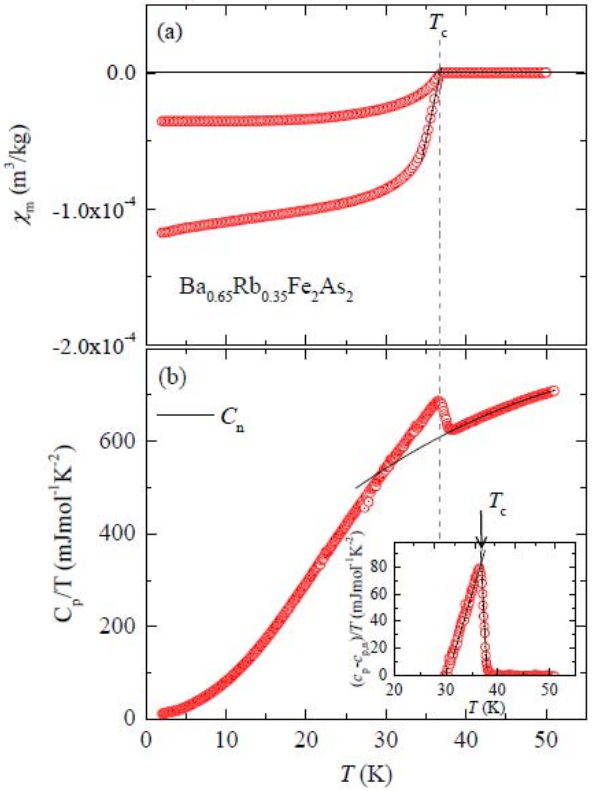

- Obtain the magnetic field penetration depth λ.
- Based on its temperature evolution one could try to speculate on the possible order parameter symmetry.

PAUL SCHERRER INSTITUT

Exercise 3 ($YBa_2Cu_3O_{7-\delta}$)

Measure the Meissner screening profile of a superconductor with Low Energy μSR

Direct measurement of the magnetic penetration depth

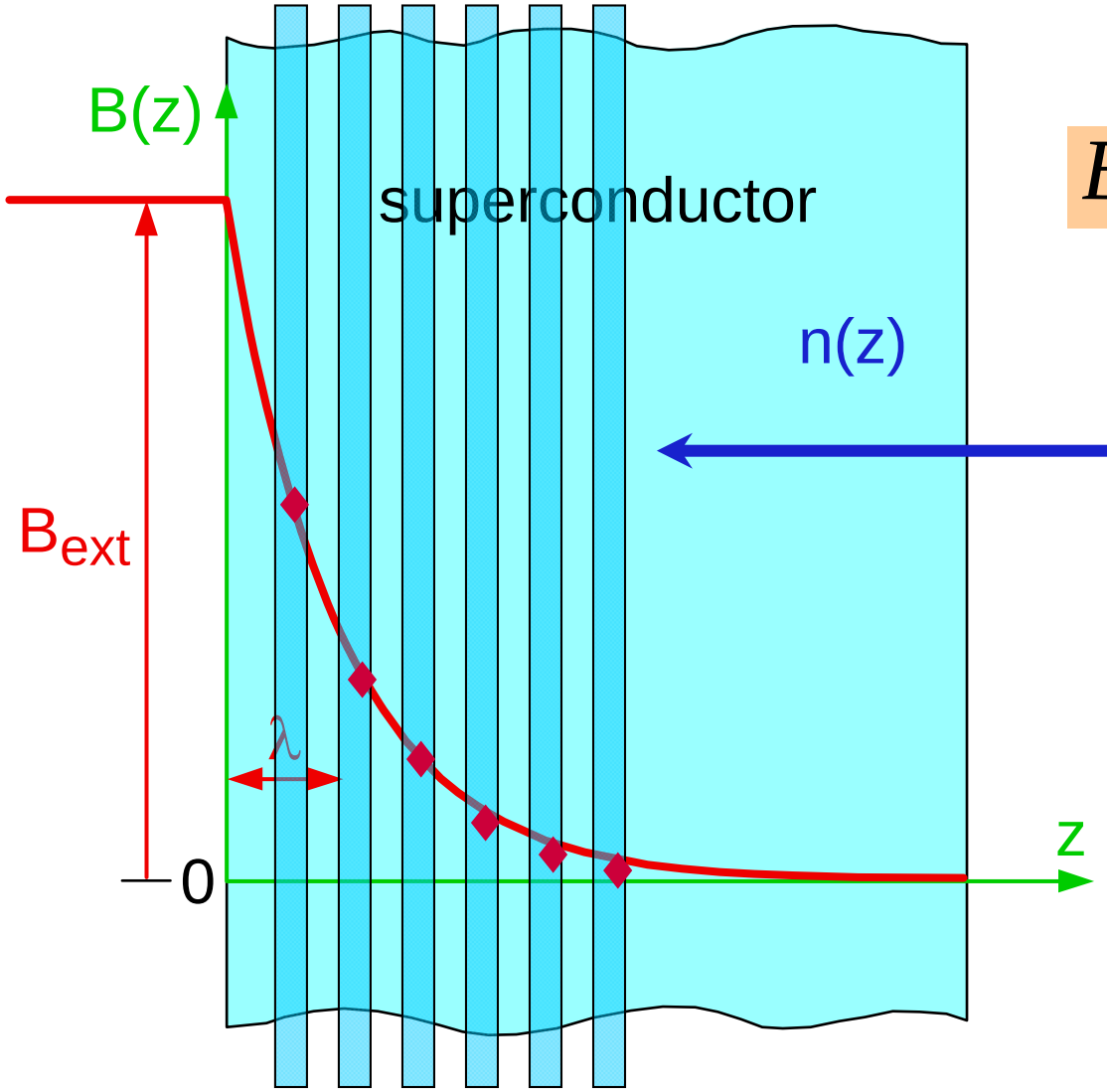

$$B(z) = B_{ext} \exp(-z/\lambda)$$

muon implantation depth profile n(z) for a particular muon energy E_μ

μSR experiment ⇒ magnetic field probability distribution p(B) at the muon site

n(z) and p(B) ⇒ B(z)

λ: magnetic penetration depth

Jackson *et al*., PRL **84**, 4958 (2000)

Direct measurement of the magnetic penetration depth

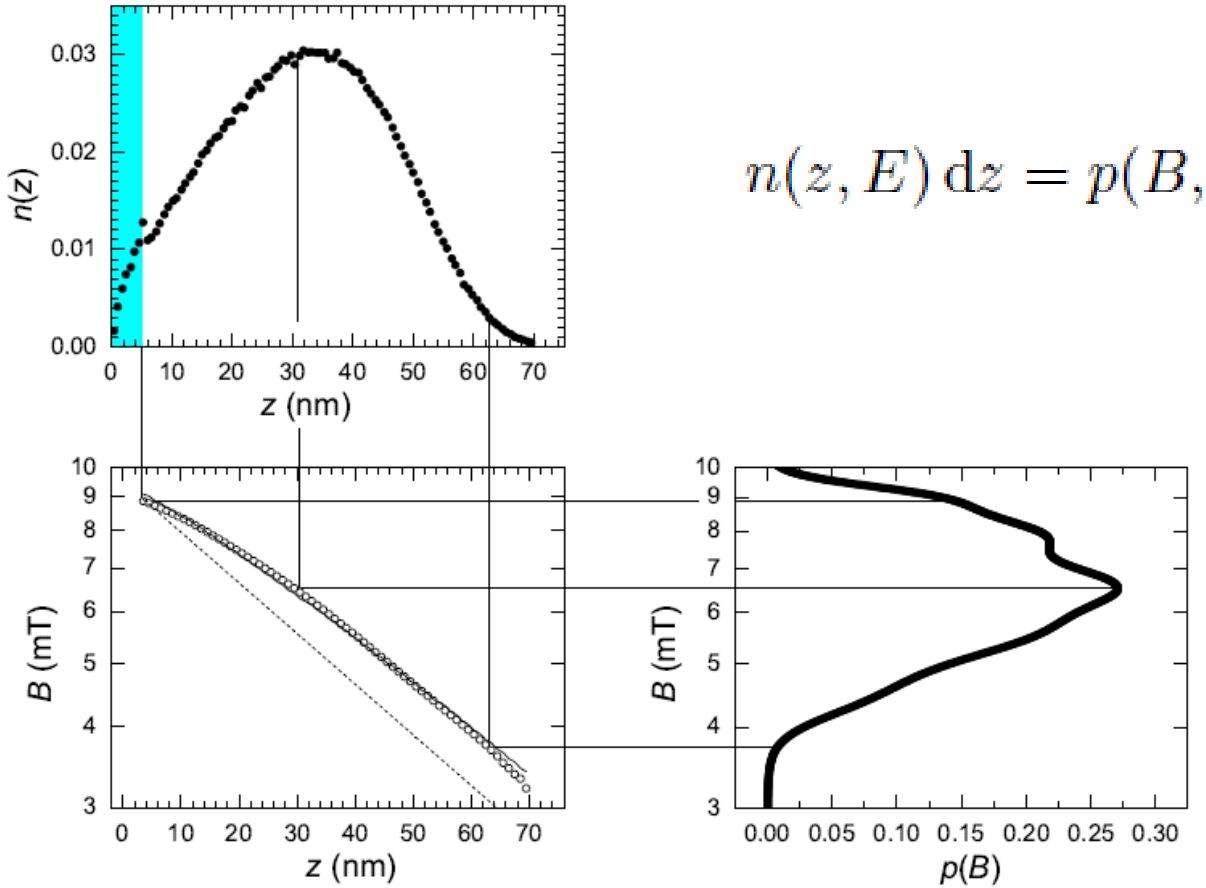

$$n(z, E)\,\mathrm{d}z = p(B, E)\,\mathrm{d}B$$

Suter PRB 72 024506 (2005)

Magnetic penetration profile B(z) in sample Pb-II at T = 3.03 K. The μ + implantation energy was E = 5.2 keV. Top graph: μ + stopping profile n(z, E) from the Monte Carlo code TRIM.SP. Bottom right graph: p(B, E) obtained from maximum entropy analysis.

Direct measurement of the magnetic penetration depth

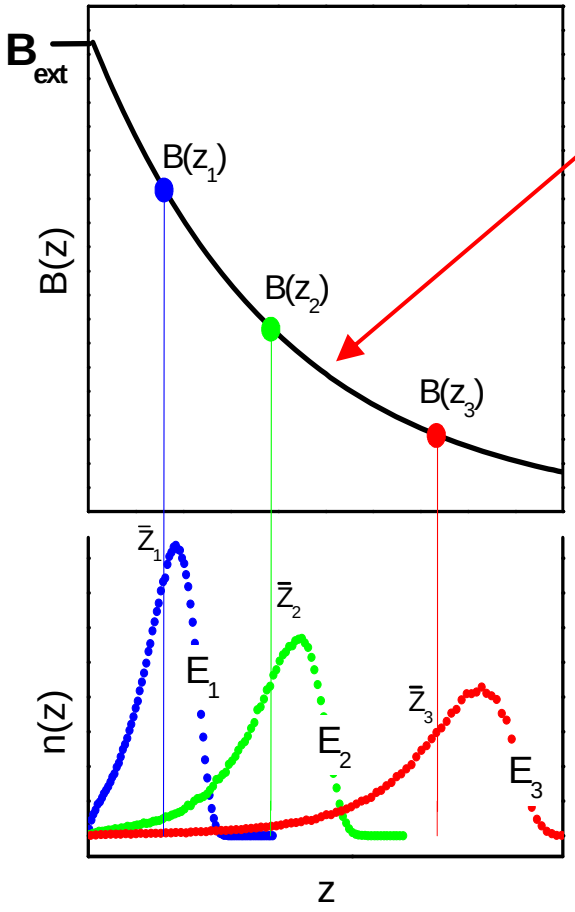

$$B(z) = B_{ext} \exp(-z/\lambda)$$

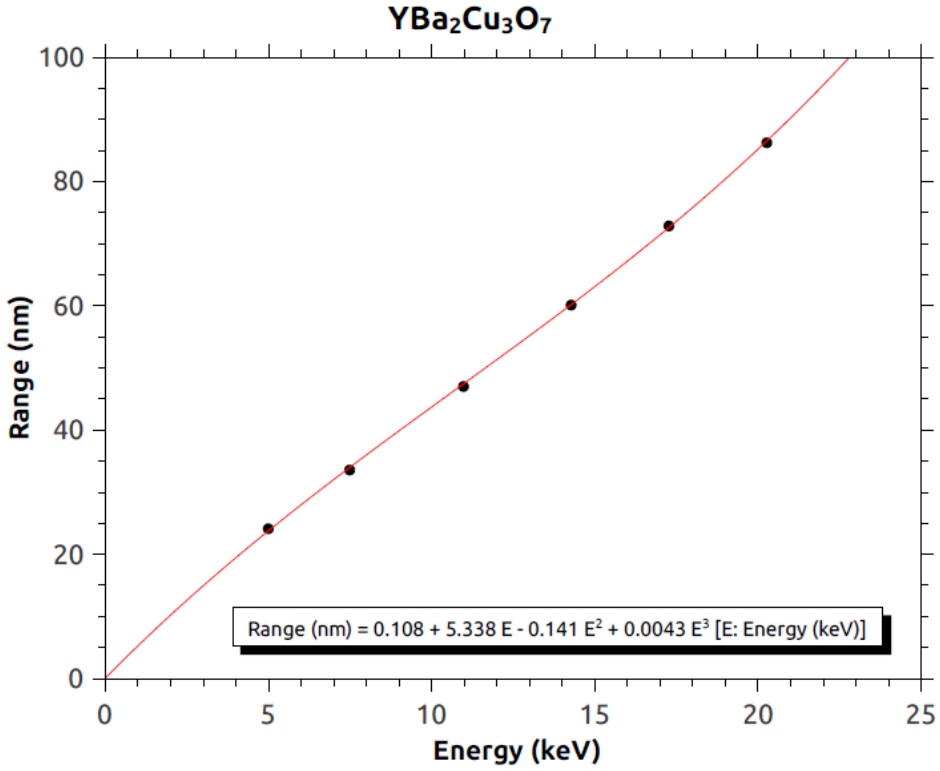

Jackson *et al.*, PRL 84, 4958 (2000)
Suter *et al.*, PRL 92, 087001 (2004)
Kiefl *et al.*, PRB 81, 180502(R) (2010)

PAUL SCHERRER INSTITUT

μSR experiments under the pressure

PAUL SCHERRER INSTITUT

SμS – The Swiss Muon Source

High Field μSR

Muon energy:
4.2 MeV (μ^+)

9.5T, 20mK

GPS

General Purpose Surface Muon Instrument
Muon energy: 4.2 MeV (μ^+)

0.6T, 1.8K

Shared Beam Surface Muon Facility
(Muon On REquest)

LTF

Low Temperature Facility
Muon energy: 4.2 MeV (μ^+)

3T, 20mK- 4K

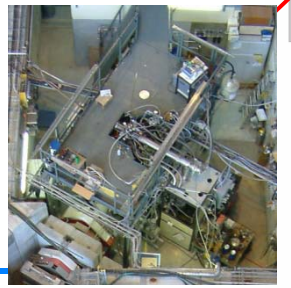

LEM

Low-energy muon beam and instrument , tunable energy (0.5-30 keV, μ^+), *thin-film, near-surface and multi-layer studies (1-300 nm)*

0.3T, 2.9K

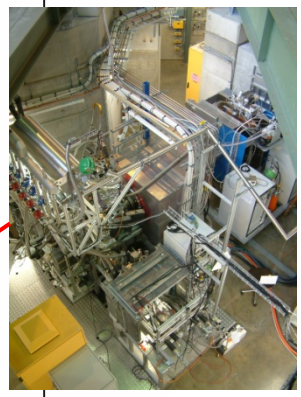

DOLLY

General Purpose Surface Muon Instrument
Muon energy: 4.2 MeV (μ^+)

0.5T, 300mK

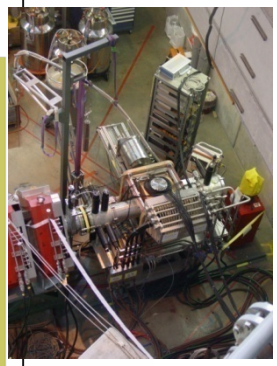

GPD

General Purpose Decay Channel Instrument
Muon energy: 5 - 60 MeV (μ^+ or μ^-)

0.5T, 300mK
2.8GPa

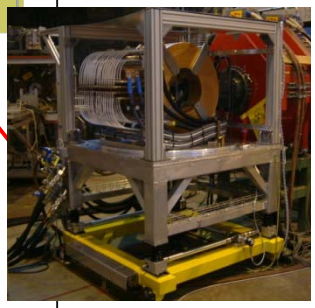

GPD spectrometer (μE1 beamline)

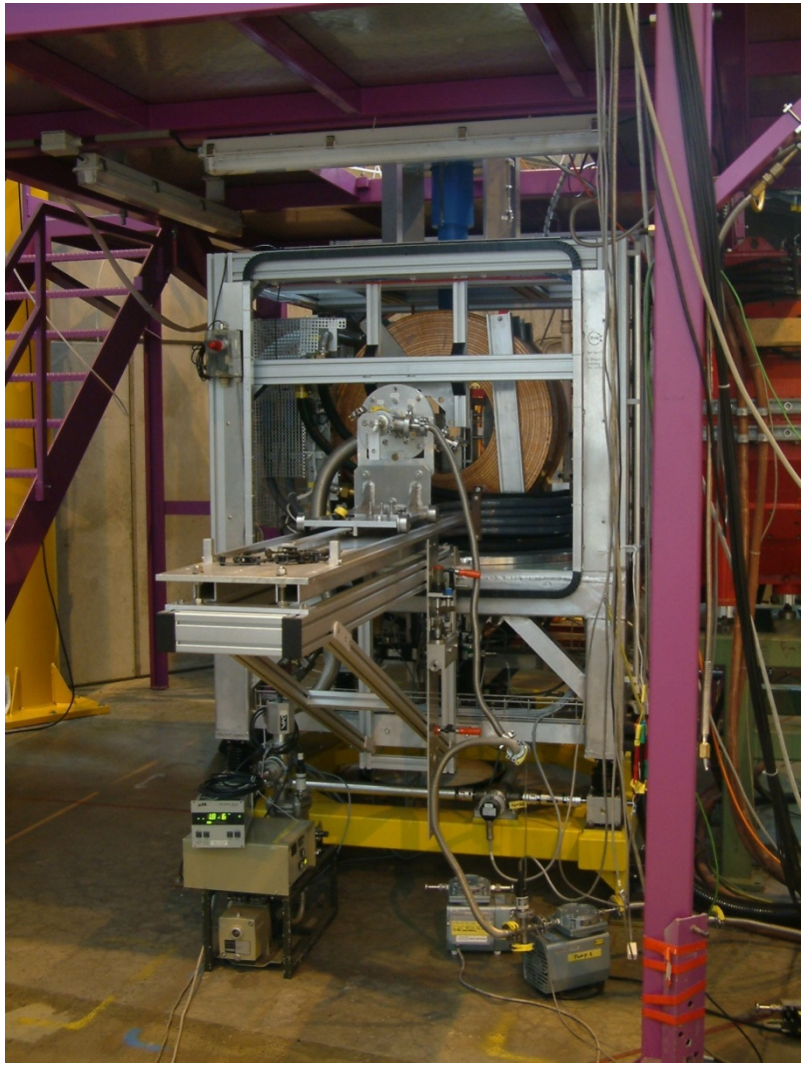

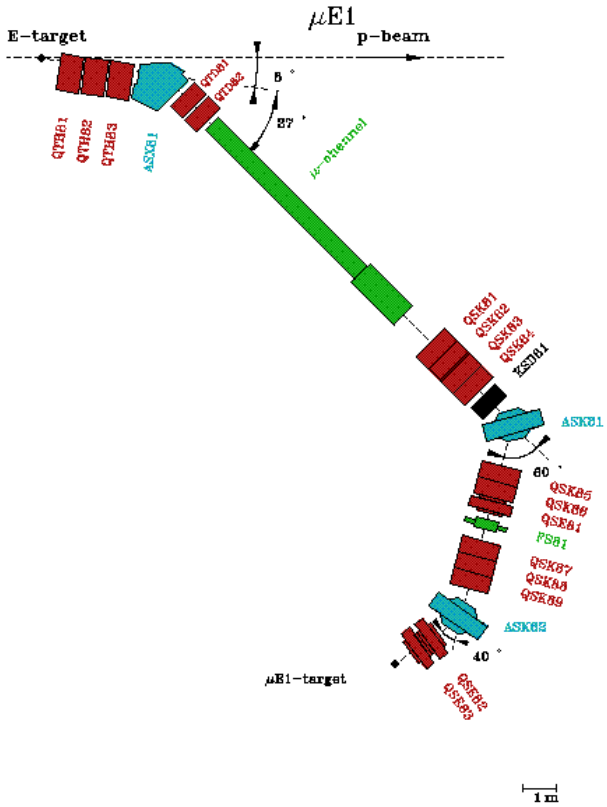

Positive or negative muons: momentum ranges ~60-125MeV/c.
Muon range: ~1.5-20g/cm2, range width ~30mg/cm2-~4g/cm2 FWHM in CH2.
Polarization: Longitudinal (direction of the muon momentum; no spin rotation).

Momentum acceptance (FWHM)	3%
Pion momentum range [MeV/c]	200--125
Muon momentum range [MeV/c]	125-- 60
Rate of positive muon [$mA^{-1}s^{-1}$]	6e7--3e7
Spot size (FWHM)	39 X 28 mm

μSR under pressure

Pressure cell

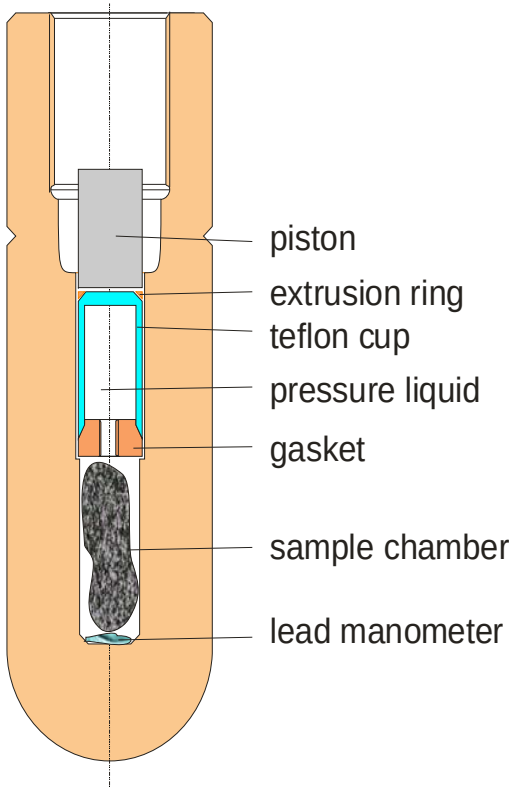

Material: CuBe, MP35N
Pressure range: up to ~2.1GPa (normal operation)
Temperature range: 0.25K—300K

AC cryostat

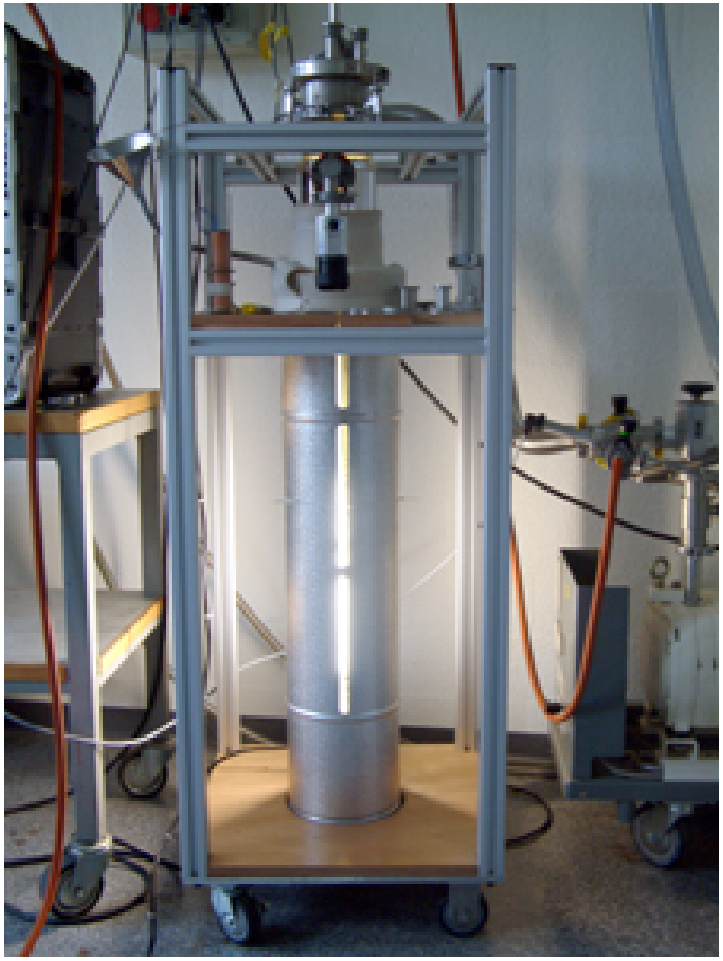

Pressure measurements

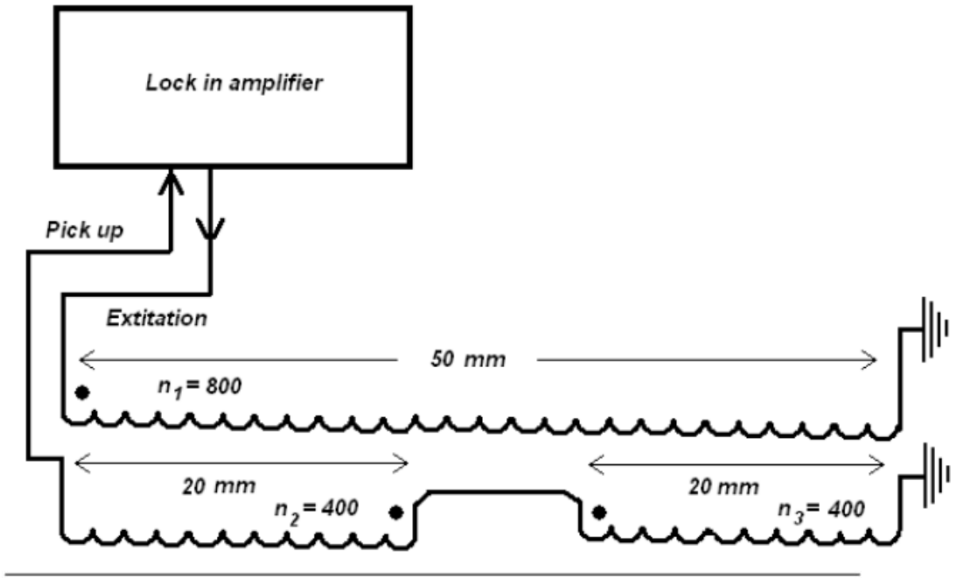

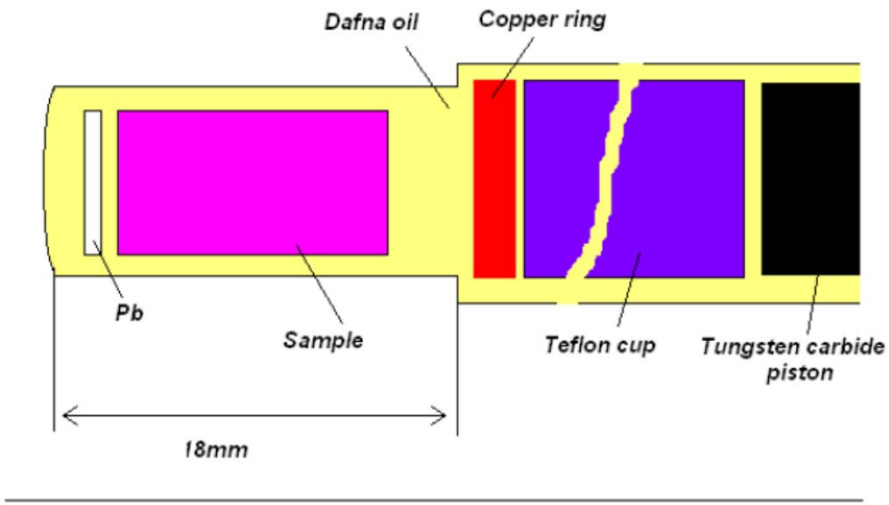

Double-wall pressure cell

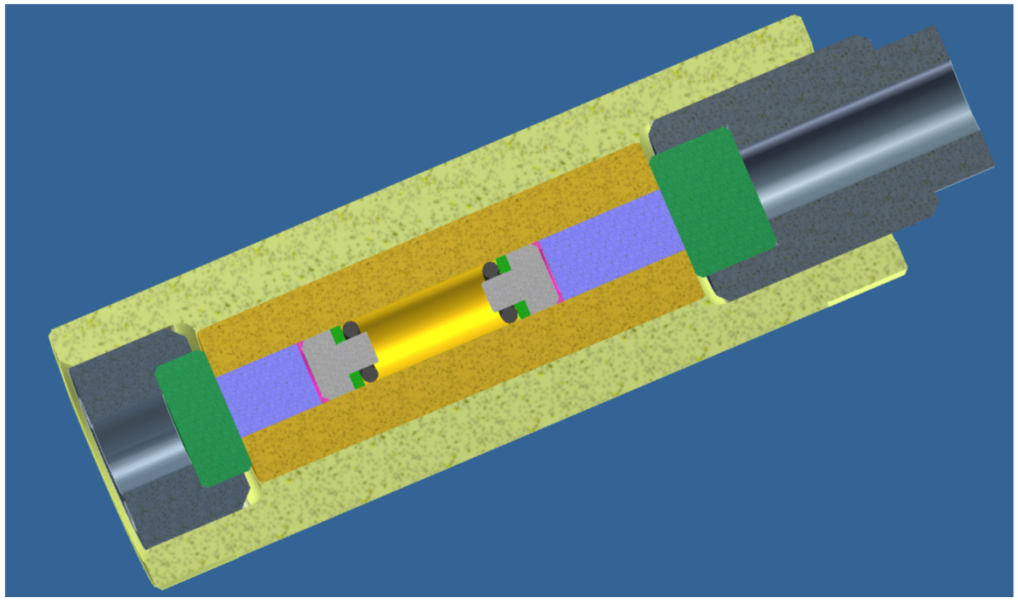

- Maximum pressure: ~2.8 GPa @ T~4K (~4GPa @ RT)
- Pressure cell size: 26mm in diameter 72 mm height
- Pressure media: Daphne oil 7373
- Sample size: 6 mm in diameter 12mm height
- Muon stopping fraction: 50-55%

Pressure beam time at PSI

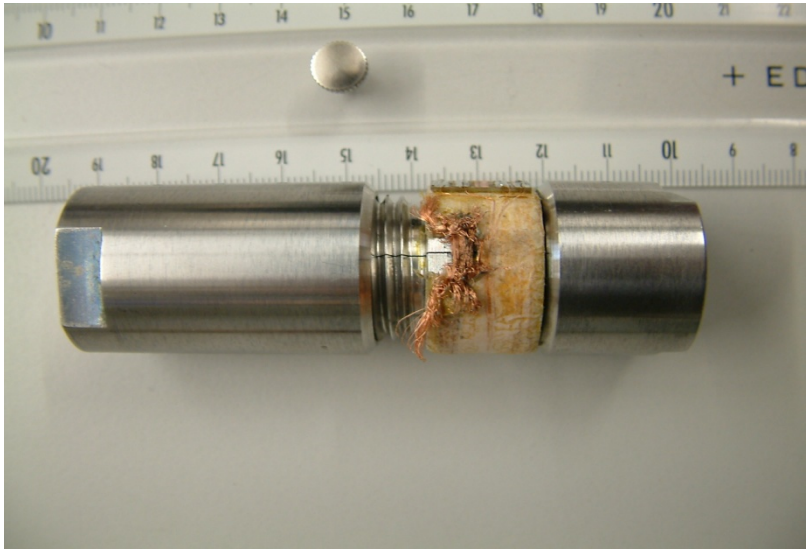

PAUL SCHERRER INSTITUT

Pressure induced electronic phase separation in CrAs

Muon Spin Rotation / Relaxation (μSR)

Magnetism:

- Local probe
  - Magnetic volume fraction
- μSR frequency
  - Magnetic order parameter (10^{-3} – 10^{-4} μ_B)
  - Temperature dependence
- μSR relaxation rate
  - Homogeneity of magnetism
- Magnetic fluctuations
  - Time window: 10^5 – 10^9 Hz

Superconductivity:

- Field distribution of vortex lattice
  - Penetration depth
  - Coherence length
  - Vortex dynamics
- Absolute determination of penetration depth $\lambda(0)$
- Temperature dependency of
  - Penetration depth, $\lambda^{-4} \propto \langle \Delta B^2 \rangle^2 \propto \sigma^2$
  - Superfluid density $n_s/m^* \propto \langle \Delta B^2 \rangle \propto \sigma$

  → Symmetry of the SC gap function

Concluding slide of Hubertus Luetkens

PAUL SCHERRER INSTITUT

CrAs crystal structure

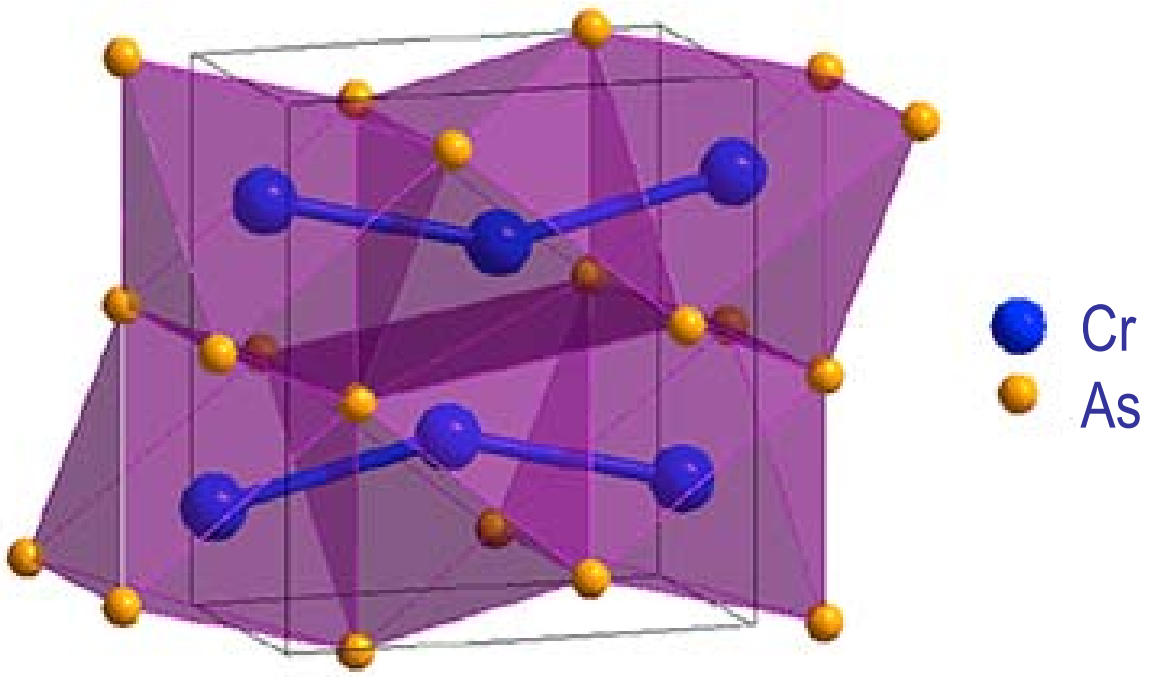

TABLE I. Refined structural and magnetic parameters of CrAs at $T = 1.5$, 80, and 300 K at ambient pressure; a–c: lattice parameters; x, z: atomic coordinates for site 4c in *Pnma*; B: temperature factor; μ: ordered magnetic moment; ϕ: magnetic phase angle; k_c: component of magnetic propagation vector.

	1.5 K	80 K	300 K
a (Å)	5.6049(3)	5.6068(3)	5.6472(3)
b (Å)	3.5852(2)	3.5846(2)	3.4727(2)
c (Å)	6.1301(5)	6.1304(4)	6.2017(6)
x/Cr (Å)	0.0068(12)	0.0064(12)	0.0060(10)
z/Cr (Å)	0.2034(10)	0.2026(8))	0.2022(10)
B/Cr (Å^2)	0.20(8)	0.32(7)	0.62(8)
x/As (Å)	0.2011(10)	0.2033(14)	0.2021(13)
z/As (Å)	0.5802(12)	0.5792(12)	0.5758(10)
B/As (Å^2)	0.12(5)	0.26(7)	0.51(7)
μ (μ_B)	1.73(2)	1.71(2)	
ϕ (°)	–110(4)	–108(4)	
k_c	0.3562(2)	0.3590(2)	
R_p	5.92	5.83	5.89

Keller *et al.*, PRB 91, 020409(R) (2015)

CrAs magnetic structure

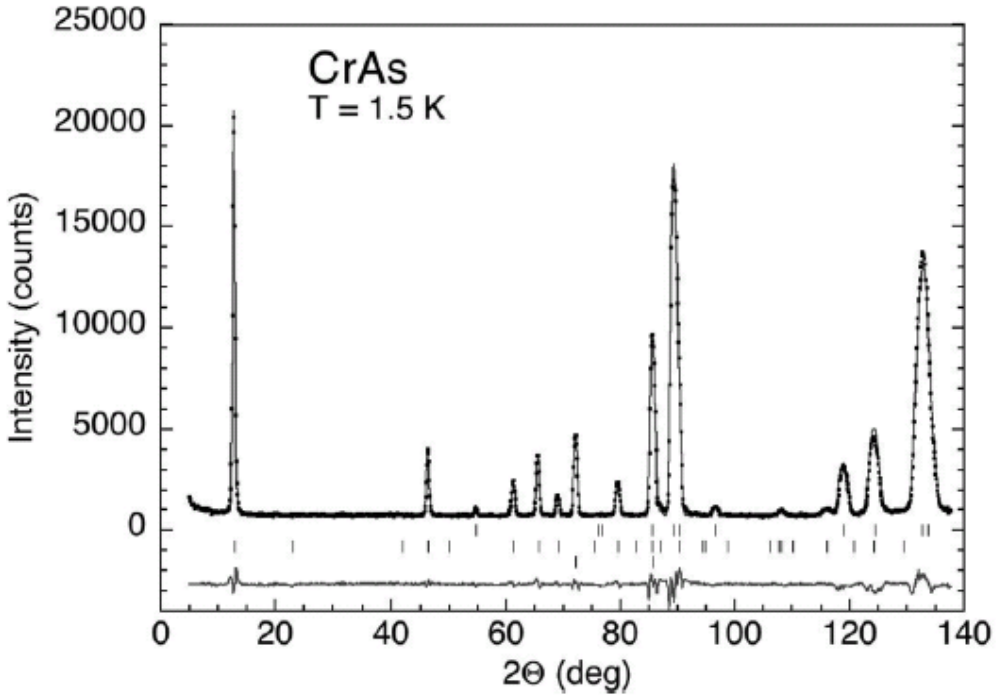

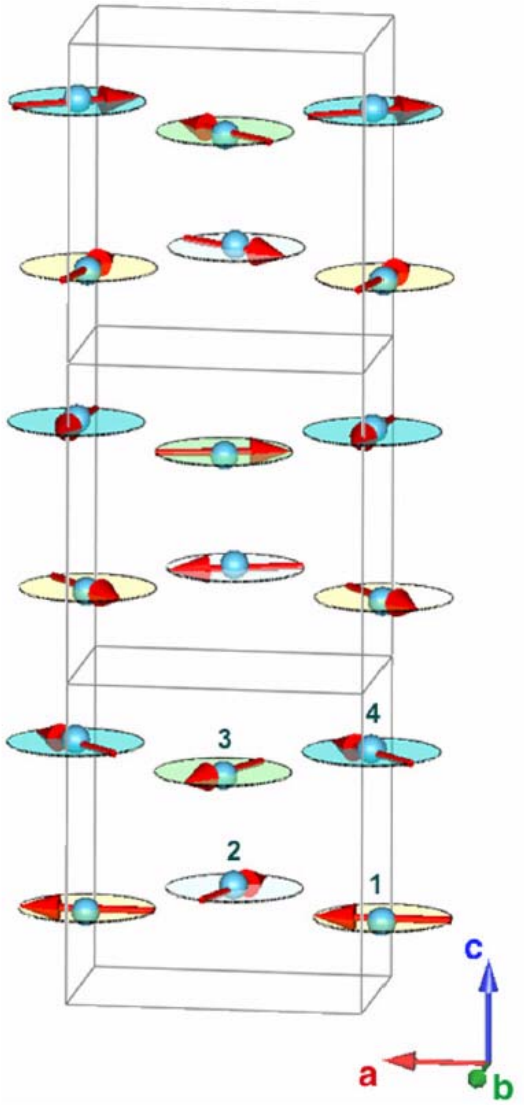

Incommensurate helical magnetic structure. The evolution of the moments for three unit cells along *c*; the four spirals are marked in individual colors. The propagation vector k_c=0.3562(2) φ is defined as the angle between the moments of Cr atoms 1 and 2 (or 3 and 4). Ordering temperature T_N=265K.

Keller *et al.*, PRB 91, 020409(R) (2015)

Pressure induced superconductivity in CrAs

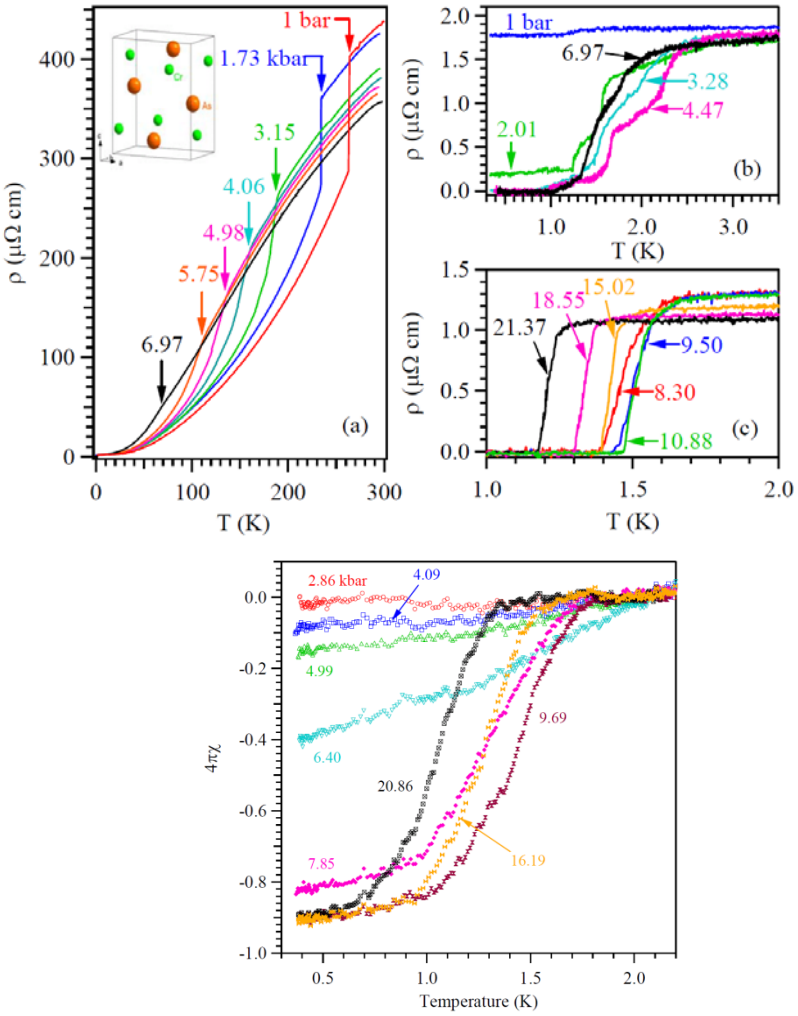

Wu *et al.*, Nat. Comm. 5, 5508 (2014)

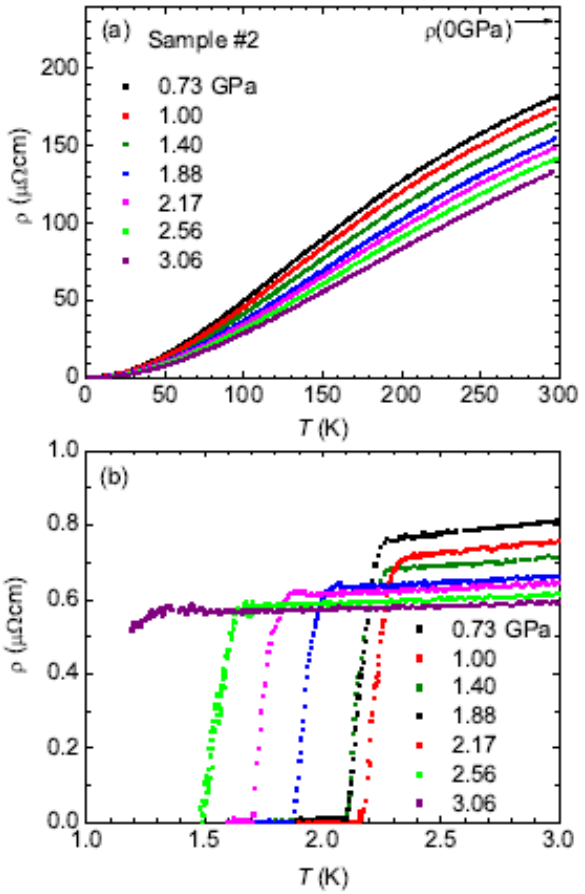

Kotegawa *et al.*, PRL 114, 117007 (2015)

Proposed phase diagrams

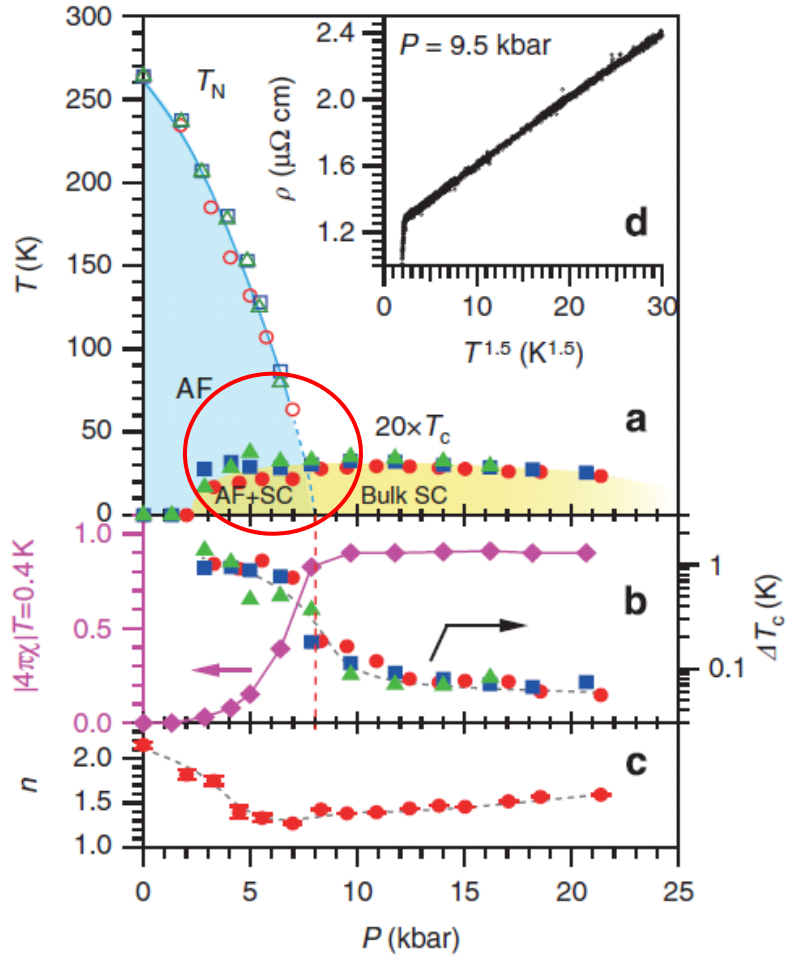

Wu *et al.*, Nat. Comm. 5, 5508 (2014)

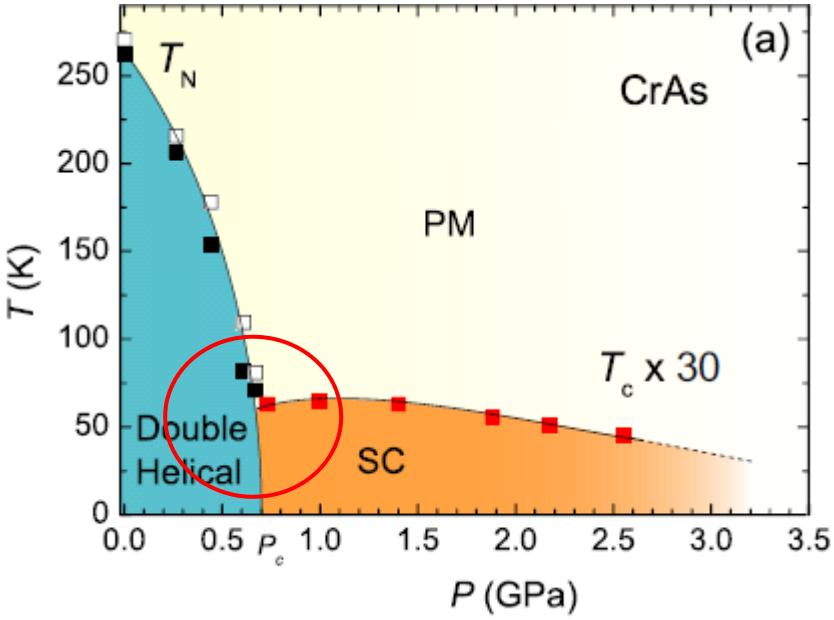

Kotegawa *et al.*, PRL 114, 117007 (2015)

Unanswered questions

1. How magnetism is suppressed?
2. How occurs the superconductivity?
3. Is there any coexistence/interplay between these two phenomena?

PAUL SCHERRER INSTITUT

Magnetic response of CrAs

(ZF and WTF experiments)

Magnetically Inhomogeneous Materials

Homogen:

M_{hom}

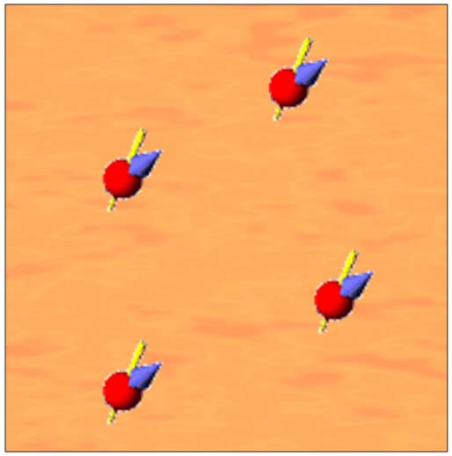

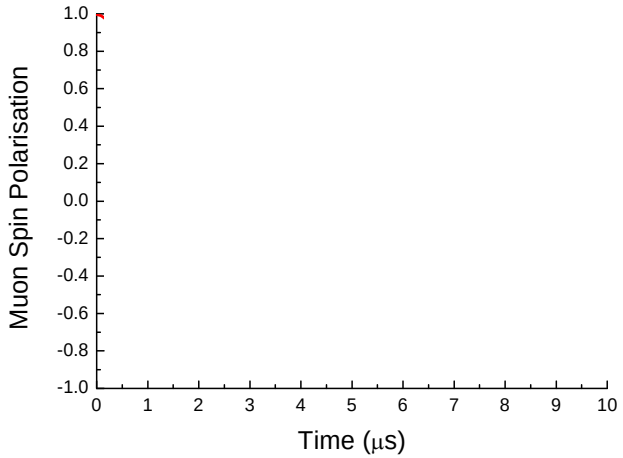

Inhomo-
geneous:

$M_{inhom} = M_{hom}$

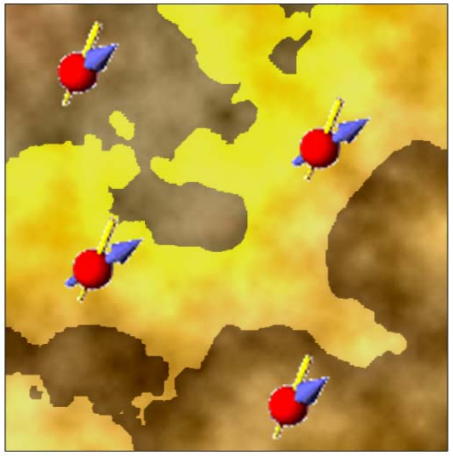

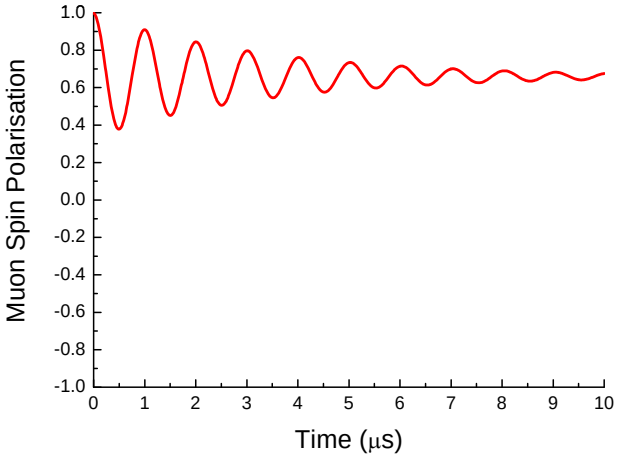

Amplitude = Magnetic volume fraction
Frequency = Size of the magnetic moments (order parameter)
Damping = Inhomogeneity within the magnetic areas

Simple Magnetic Sample – Polycrystal

$$P_z(t) = \int f(\mathbf{B}_\mu)\left[\cos^2\theta + \sin^2\theta\cos(\gamma_\mu B_\mu t)\right] d\mathbf{B}_\mu$$

Polycrystal (powder)

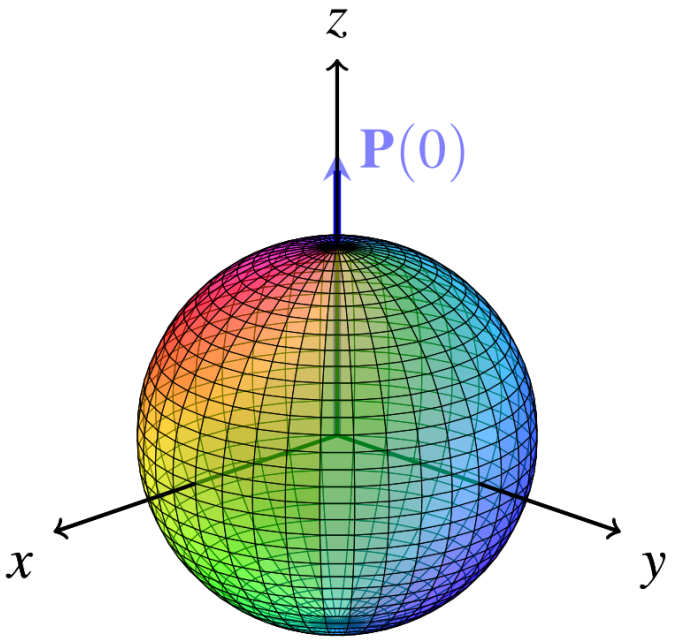

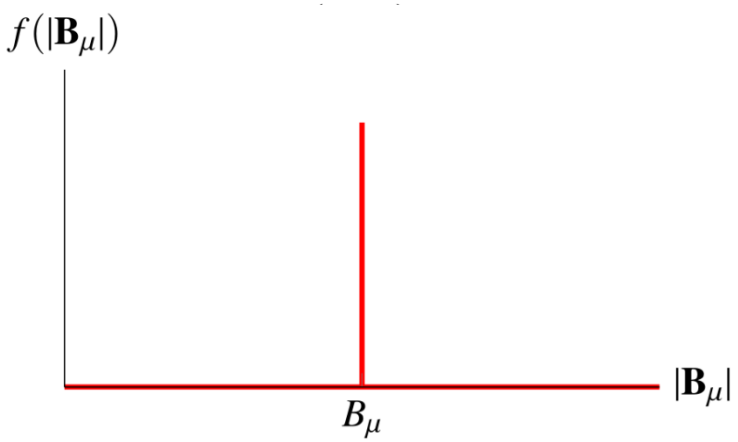

If isotropic:

$$f(|\mathbf{B}_\mu|) = f(\mathbf{B}_\mu)\, 4\pi B_\mu^2$$

$$f(\mathbf{B}_\mu)\, d\mathbf{B}_\mu = \frac{f(|\mathbf{B}_\mu|)}{4\pi}\sin(\theta)\, d\theta\, d\phi\, dB_\mu$$

$$P_z(t) = \frac{1}{3} + \frac{2}{3}\cos(\gamma_\mu\, B_\mu t)$$

After H. Luetkens (Sunday 16 Aug 2015)

Experiments in Zero Field

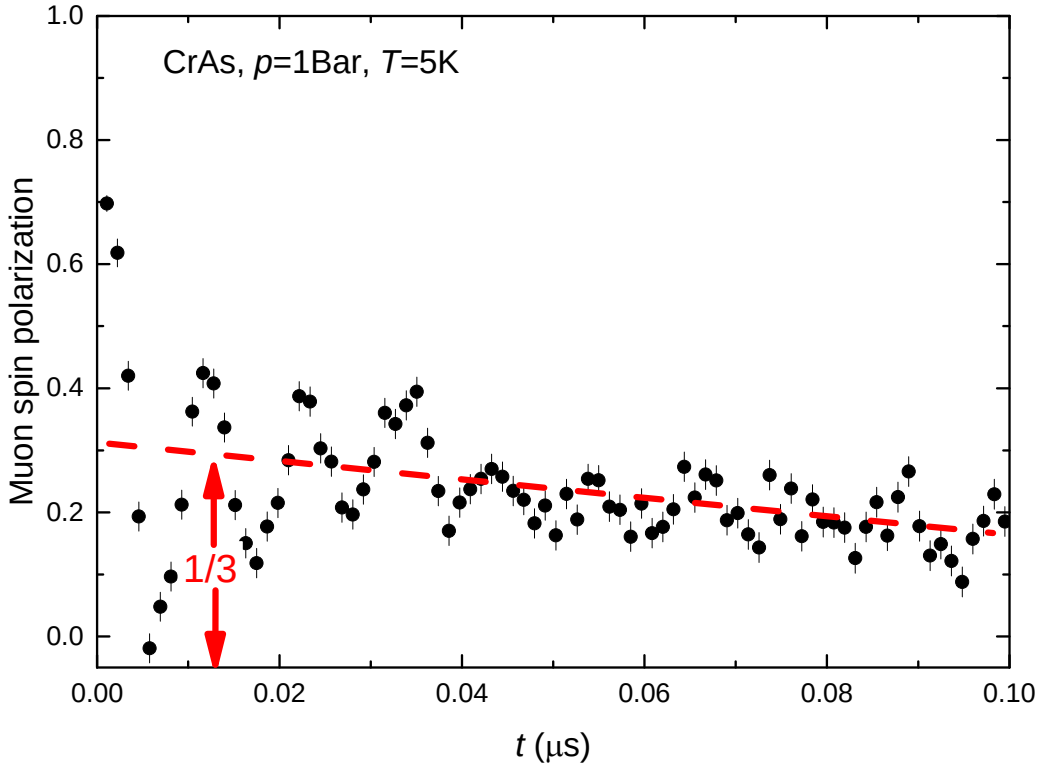

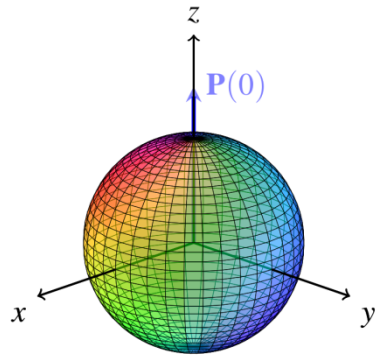

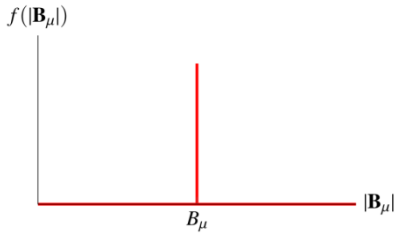

$$P_z(t) = \frac{1}{3} + \frac{2}{3}\cos(\gamma_\mu B_\mu t)$$

At ambient pressure CrAs is 100% magnetic!

Helical magnetic order

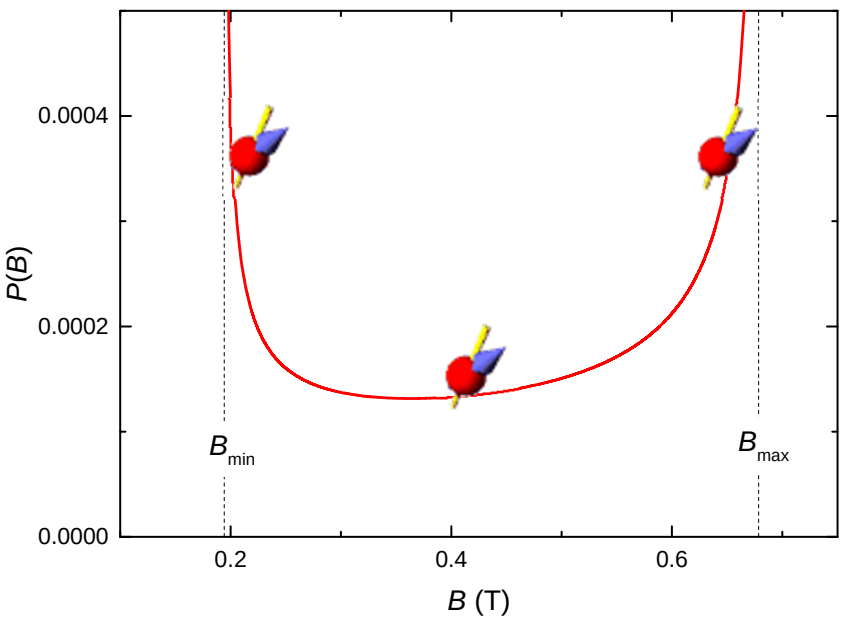

$$P(B) = \frac{2}{\pi} \frac{B}{\sqrt{(B^2 - B_{min}^2)(B_{max}^2 - B^2)}}$$

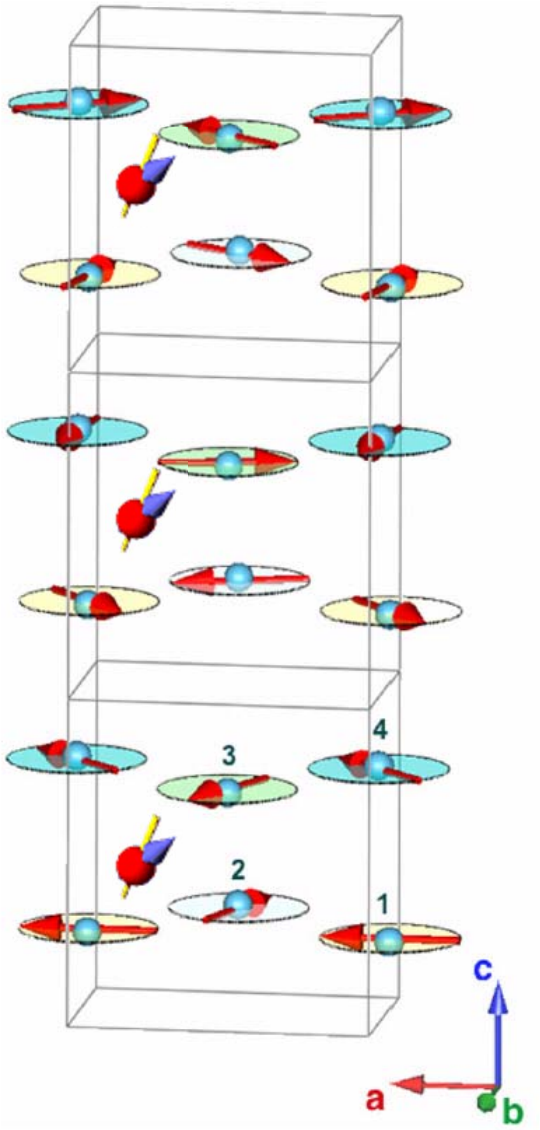

Helical magnetic order

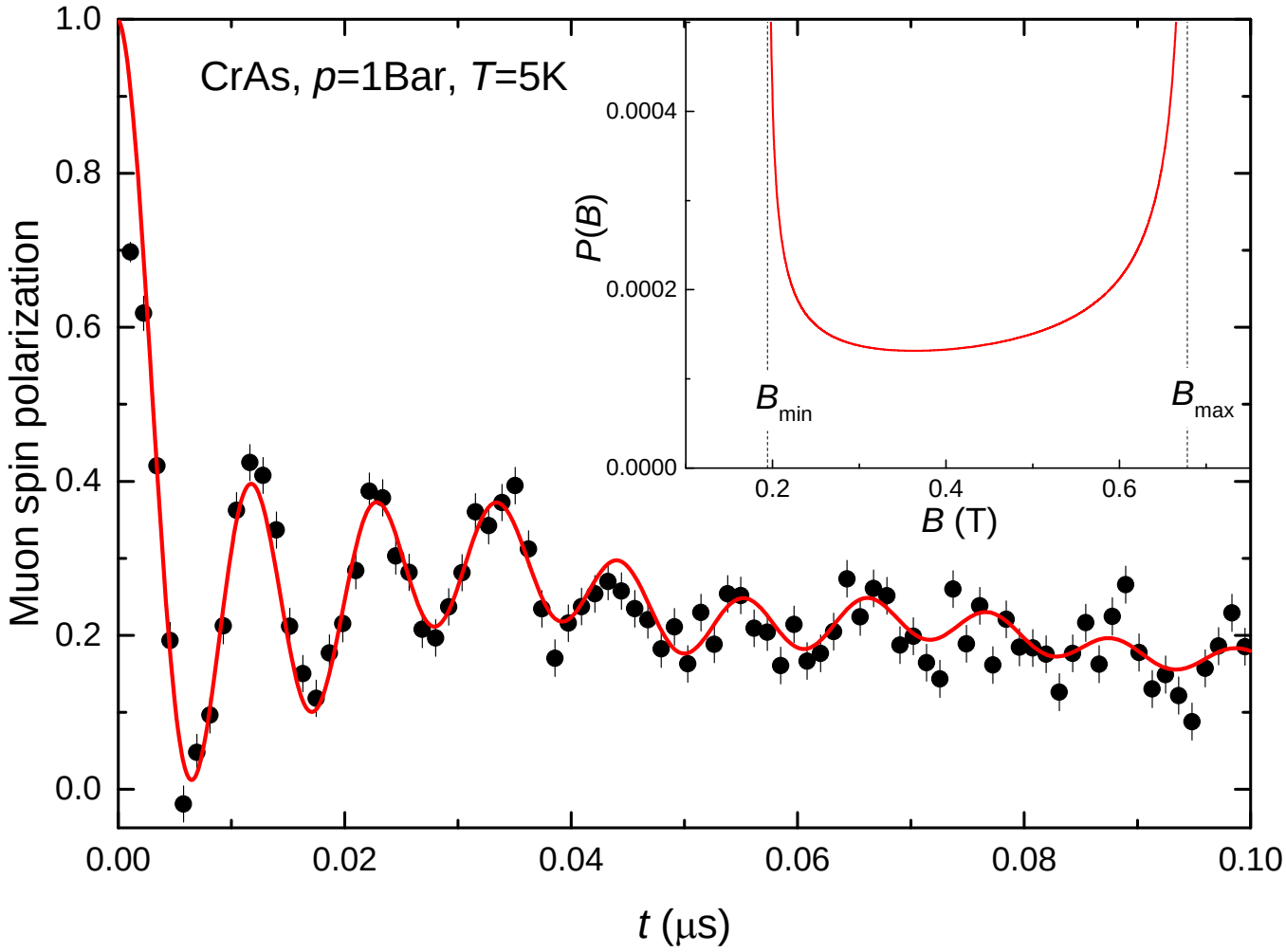

Confirmation of helical type of magnetic order in CrAs

Weak transverse field (WTF)

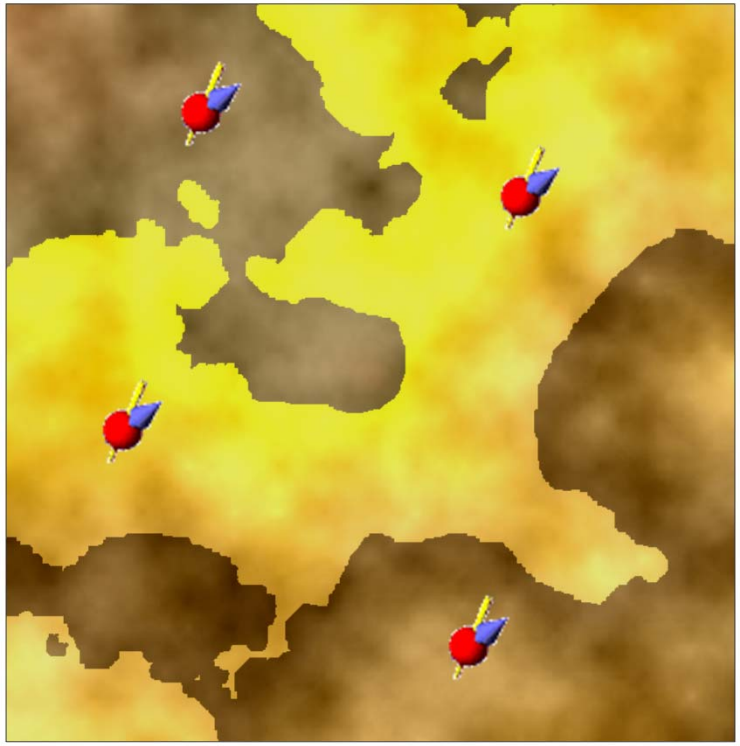

Local field at the muon stopping position is the vector sum of the "internal" ($\boldsymbol{B}_{int}$) and the "applied" ($\boldsymbol{B}_{app}$) one

$$\boldsymbol{B}_{\mu}=\boldsymbol{B}_{int}+\boldsymbol{B}_{app}$$

In a case $\boldsymbol{B}_{int}>>\boldsymbol{B}_{app}$ (weak field regime)

$\boldsymbol{B}_{\mu}=\boldsymbol{B}_{int}$ in the magnetically ordered parts

$\boldsymbol{B}_{\mu}=\boldsymbol{B}_{app}$ in paramagnetic parts

WTF experiments

WTF 3mT

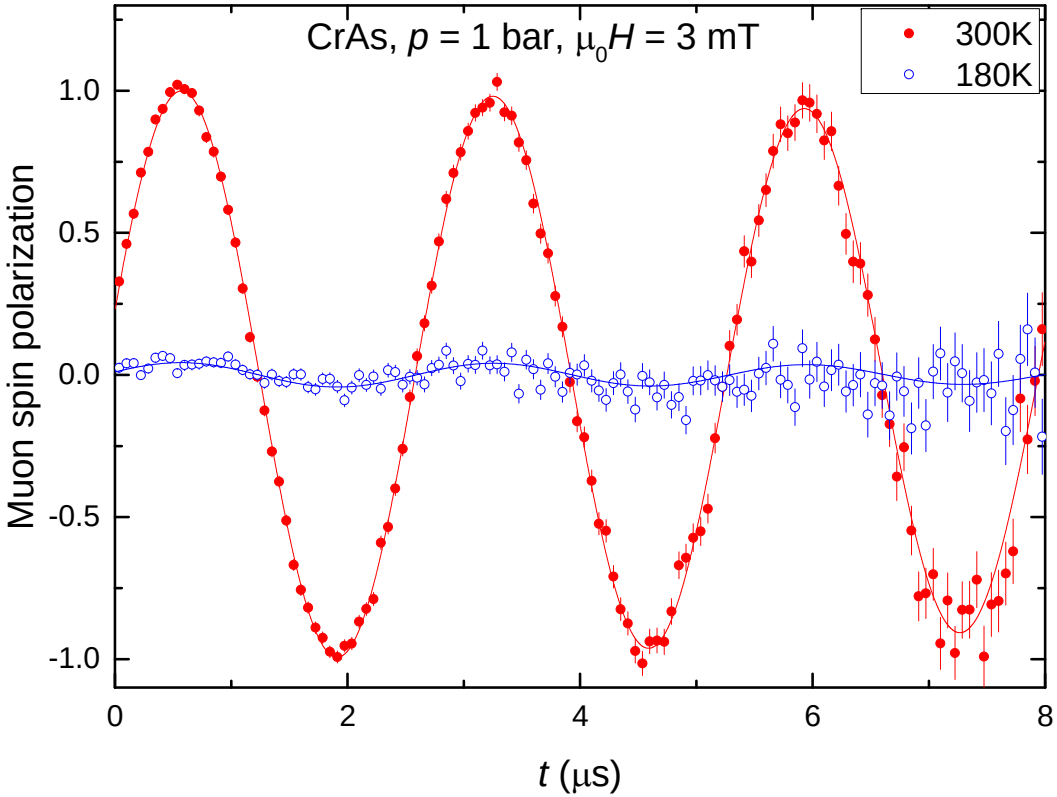

ZF

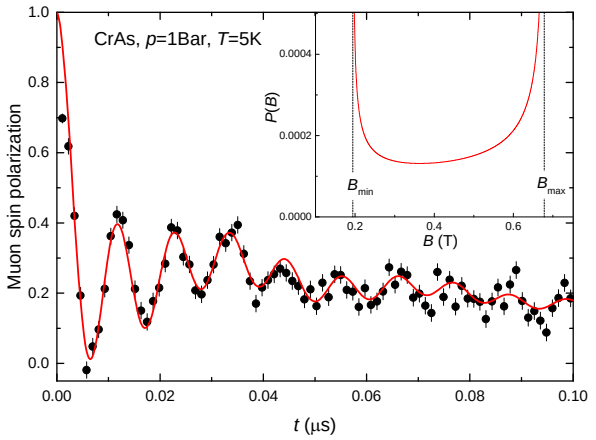

WTF experiments

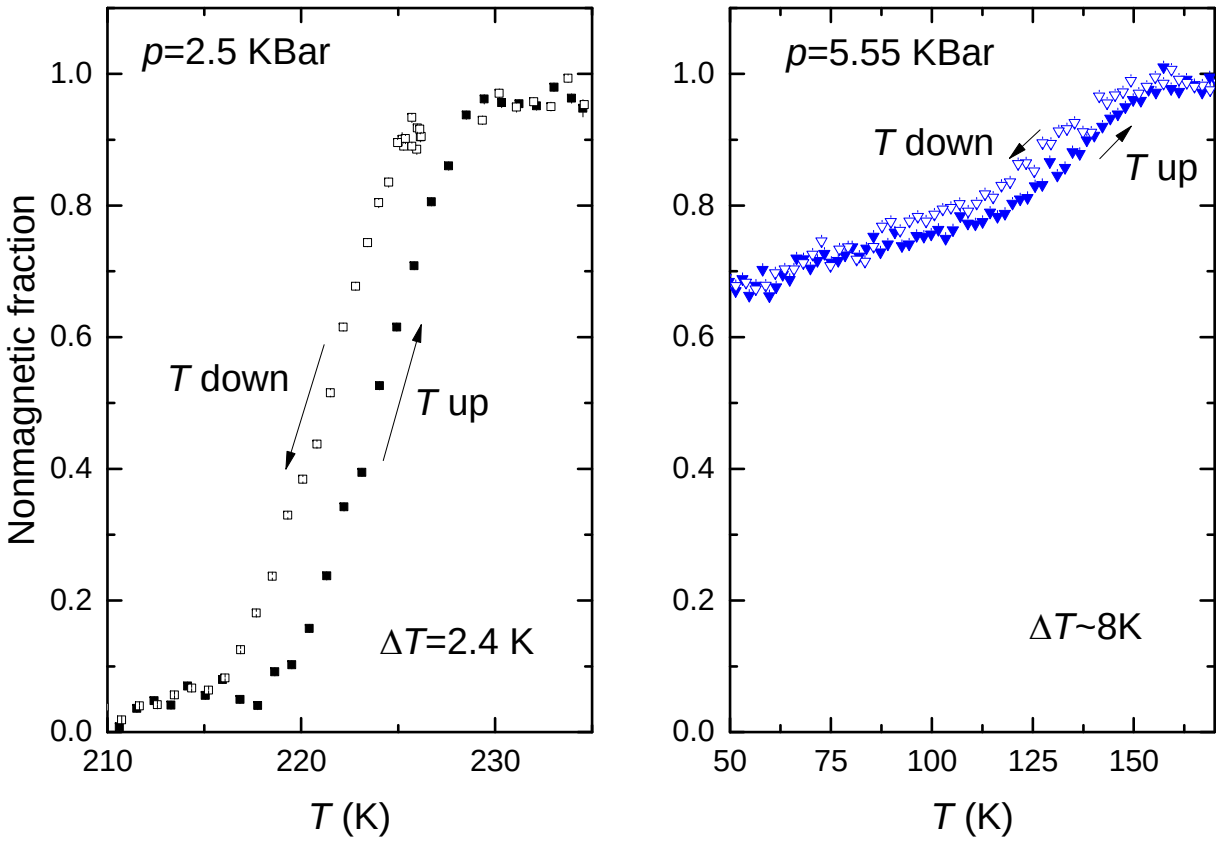

- The magnetic transition is first order like
- Transition temperature decreases with increasing pressure
- Magnetic volume fraction decreases with pressure increase

Magnetic response of CrAs

WTF

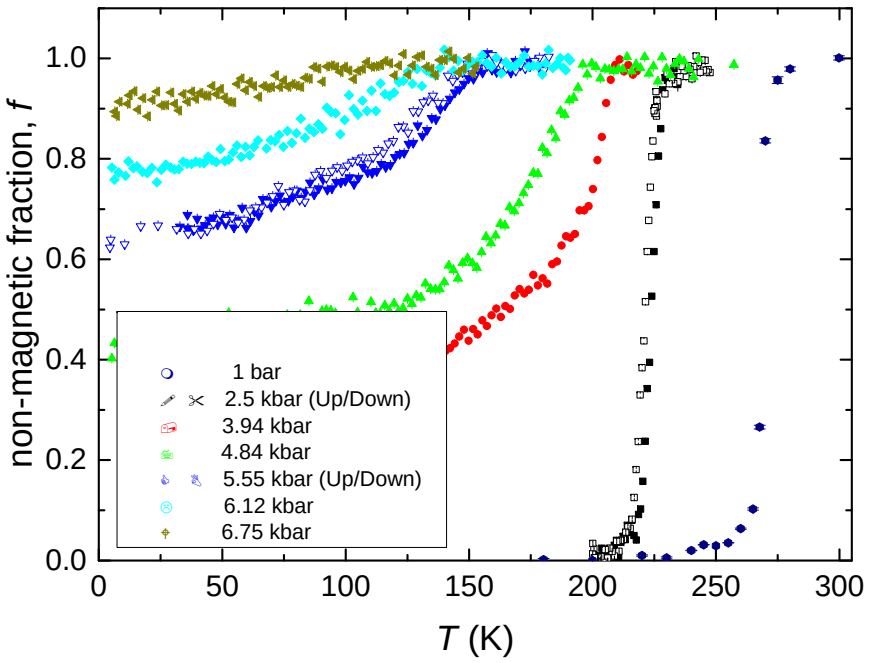

ZF

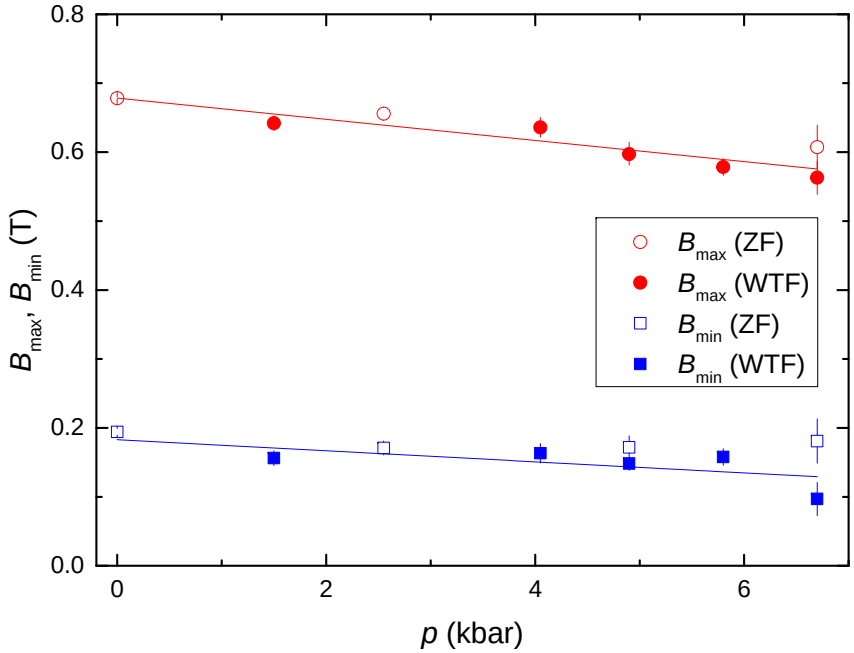

No magnetism above p~7 Kbar!

Magnetic response of CrAs

T_N

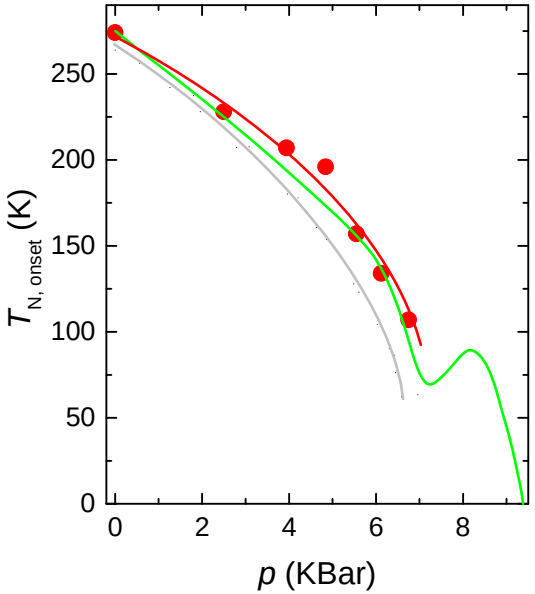

Nonmagnetic fraction

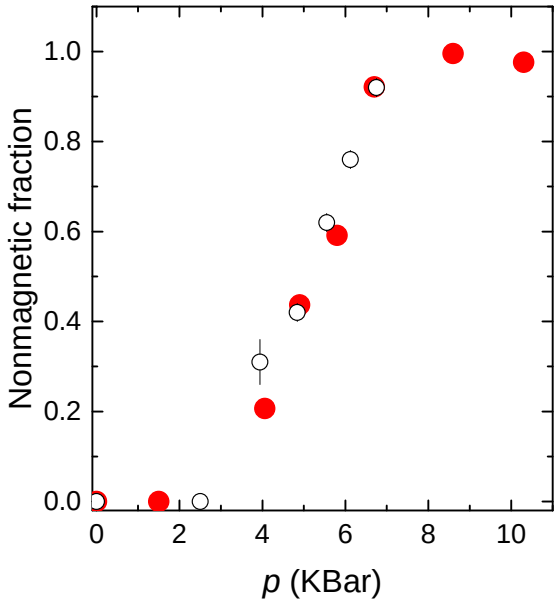

Ordered moment

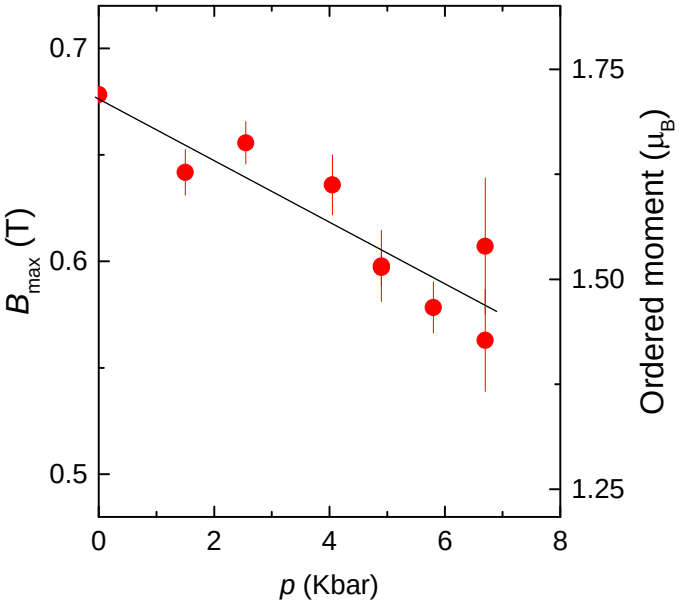

Wu *et al.*, Nat. Comm. 5, 5508 (2014)

Kotegawa *et al.*, PRL 114, 117007 (2015)

Shen *et al.*, arxiv:14083158

Comparison with neutron data

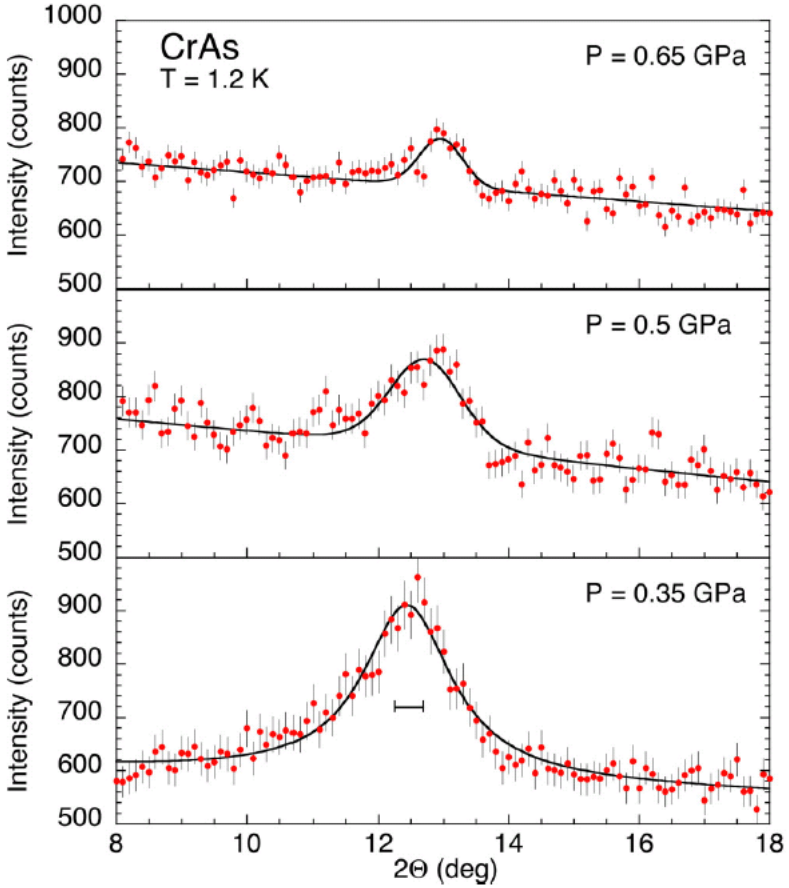

FIG. 4. (Color online) Pressure dependence of the first magnetic satellite $(00 \pm k_c)$ for the pressures $P = 0.35$, 0.5, and 0.65 GPa. A convolution of Lorentzian and Gaussian peak shape functions was used for the profile fits.

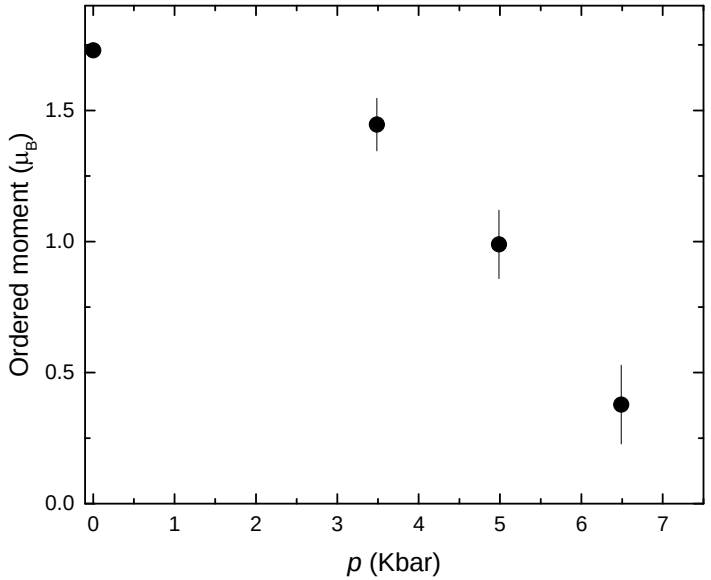

Keller *et al.*, PRB 91, 020409(R) (2015)

Comparison with neutron data

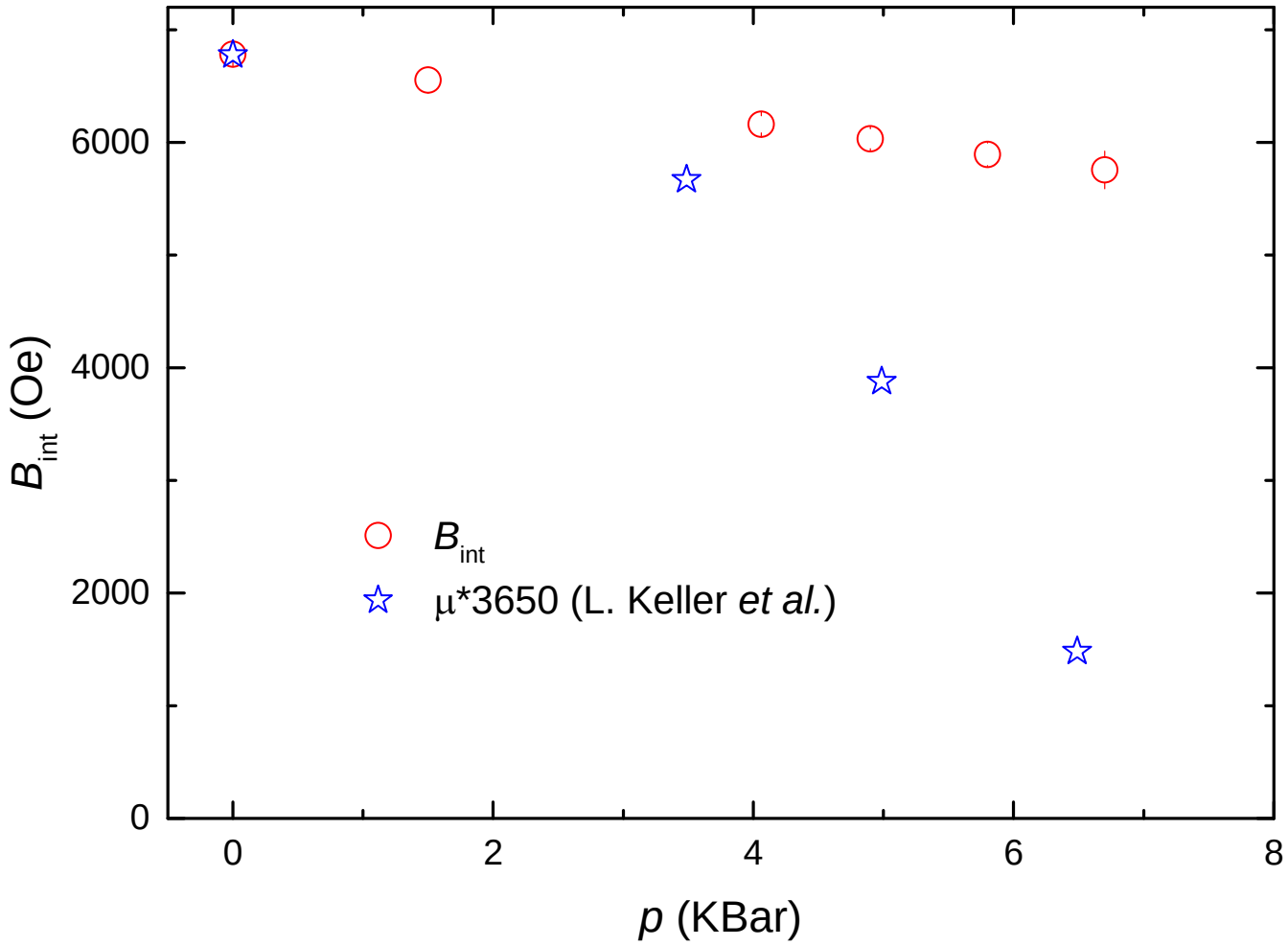

Comparison with neutron data

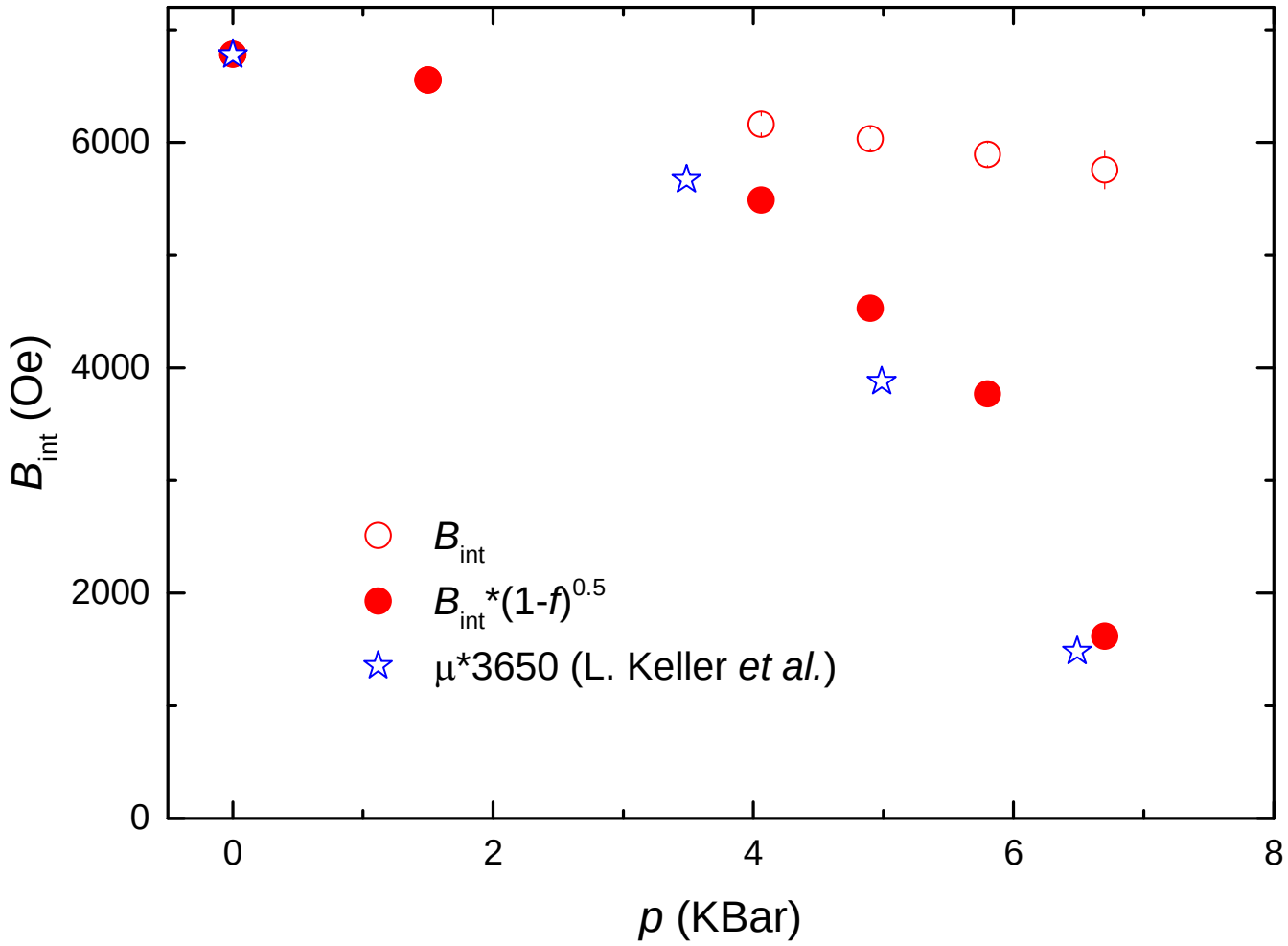

PAUL SCHERRER INSTITUT

Superconducting response of CrAs
(TF experiments)

Field Distribution in a Type II S.C.

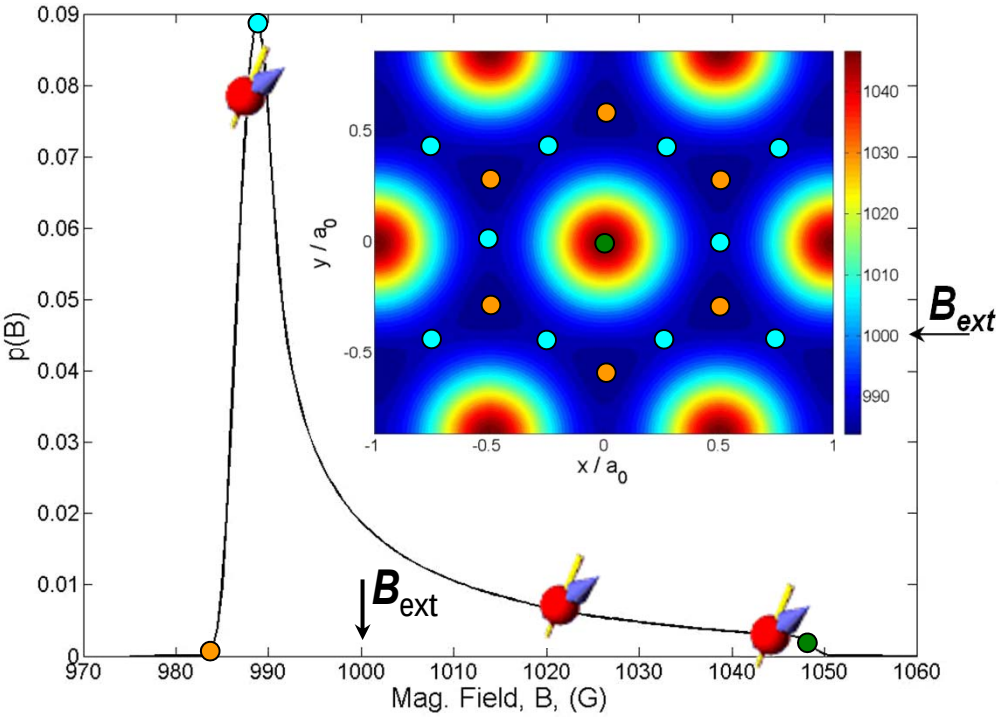

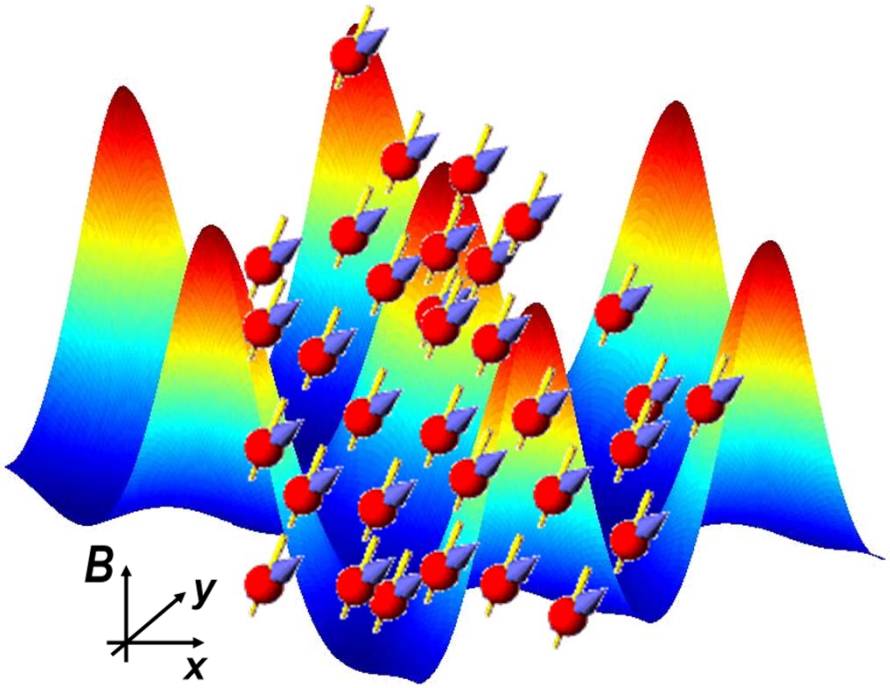

Since the muon is a local probe, the μSR relaxation function is given by the weighted sum of all oscillations:

$$G(t) = \int f(\mathbf{B}_\mu) \cos(\gamma_\mu B_\mu t) d\mathbf{B}_\mu$$

After H. Luetkens (Sunday 16 Aug 2015)

Extract Information from the μSR data

$$G(t) = \underbrace{\exp(-\frac{1}{2}\sigma^2 t^2)}_{\text{depolarization}} \times \underbrace{\cos(\gamma_\mu \langle B_\mu^z \rangle t)}_{\text{oscillations}}$$

where: $\sigma^2 = \gamma_\mu^2 \langle \Delta B_\mu^{z\,2} \rangle$

*Pümpin et al., Phys. Rev. B **42**, 8019 (1990)*

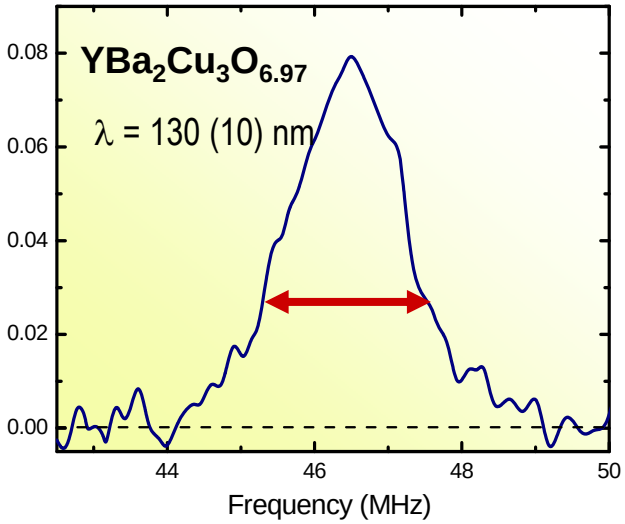

Ginzburg-Landau model

$$\langle \Delta B_z^2 \rangle = 0.00371 \frac{\phi_0^2}{\lambda^4}$$

London model

$$\lambda = \sqrt{\frac{m}{\mu_0 e^2 n_s}}$$

$$\Rightarrow \quad \sigma \propto \frac{1}{\lambda^2} \propto \frac{\mu_0 e^2}{m} n_s$$

A μSR measurement of the second moment of the field distribution allows to determine the London penetration depth λ.

The damping of a TF-μSR spectrum is proportional to the super fluid density n_s (number of Cooper pairs).

After H. Luetkens (Sunday 16 Aug 2015)

TF 30mT

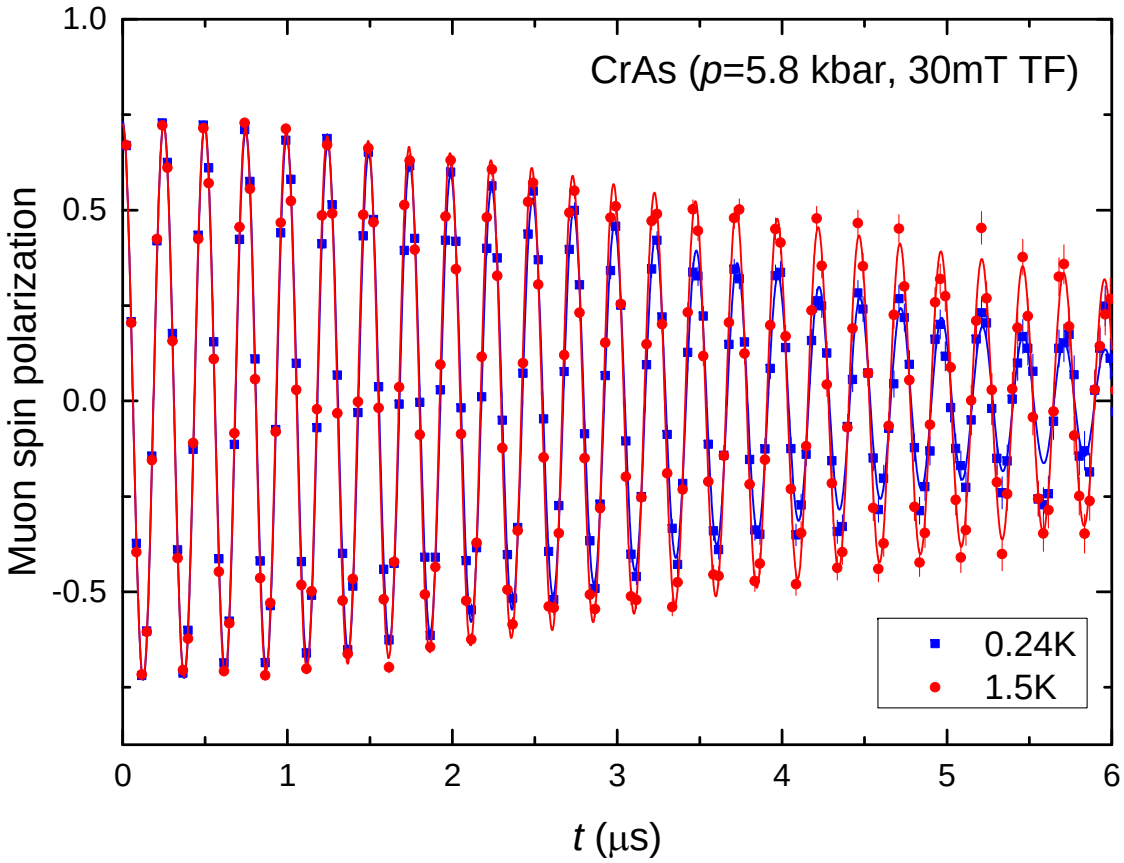

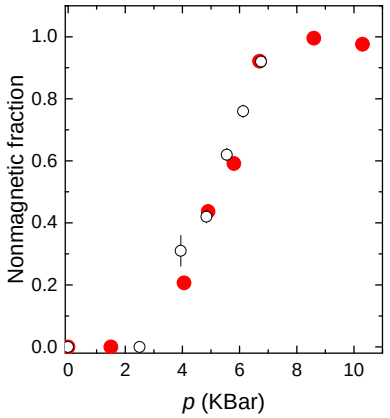

Appr. 20% of the sample remains in the magnetic state

TF 30mT

Superfluid density

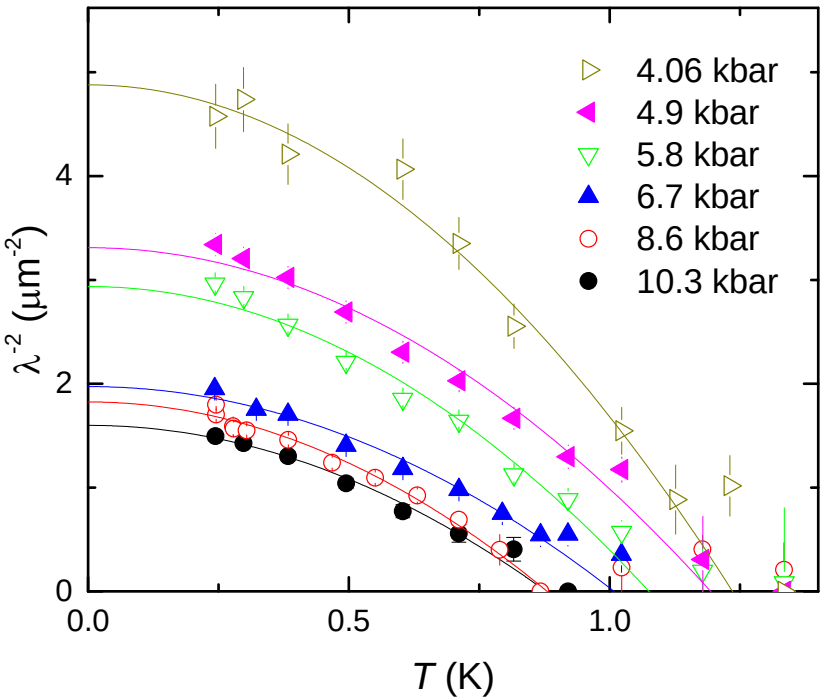

Diamagnetic shift

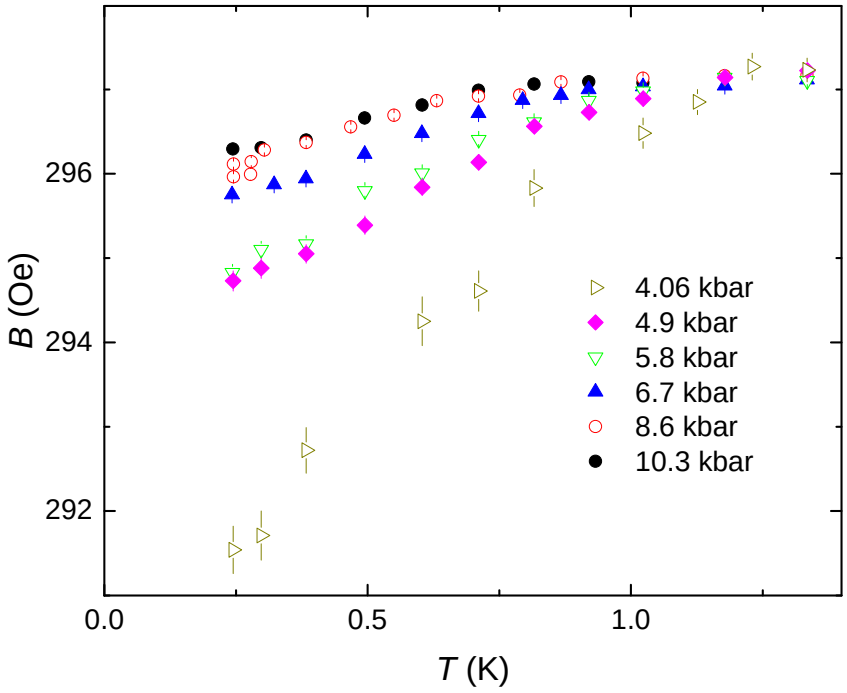

Phase coexistence in CrAs

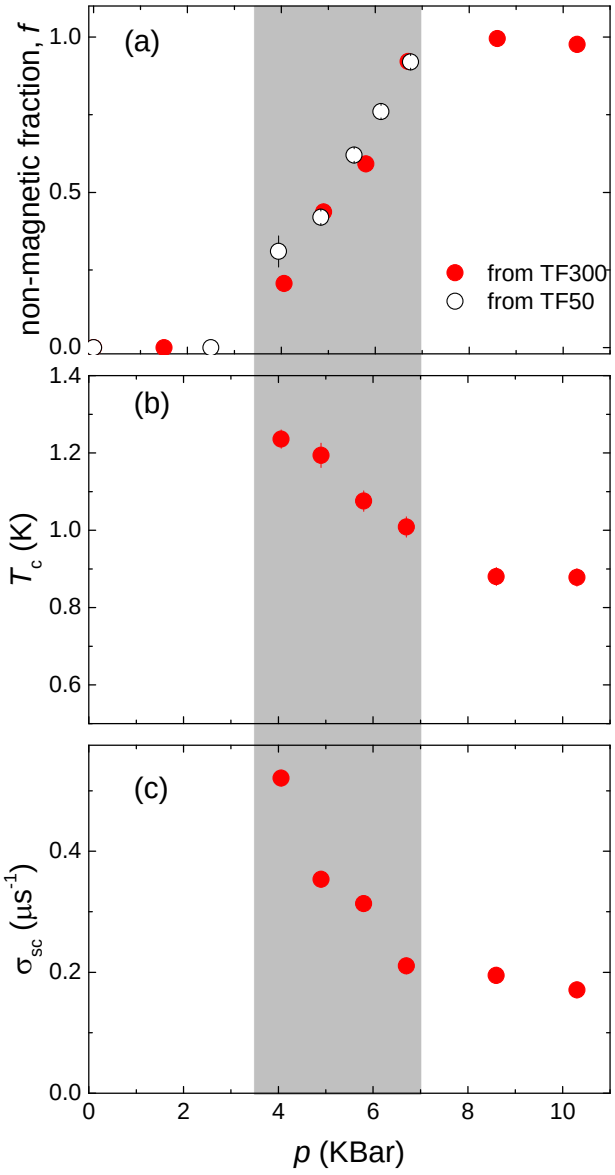

- CrAs is purely magnetic up to p~3.5kbar
- For 3.5<p<7kbar magnetic and superconducting responses are detected in a set of ZF, wTF, and TF experiments. CrAs is phase separated into volumes where long range magnetic order sets at T_N and into non-magnetic volumes becoming superconducting below T_c.
- Above 7kbar and above T_c the sample is purely in the paramagnetic state. Bulk superconductivity sets below T_c.

PAUL SCHERRER INSTITUT

Self-doping effect

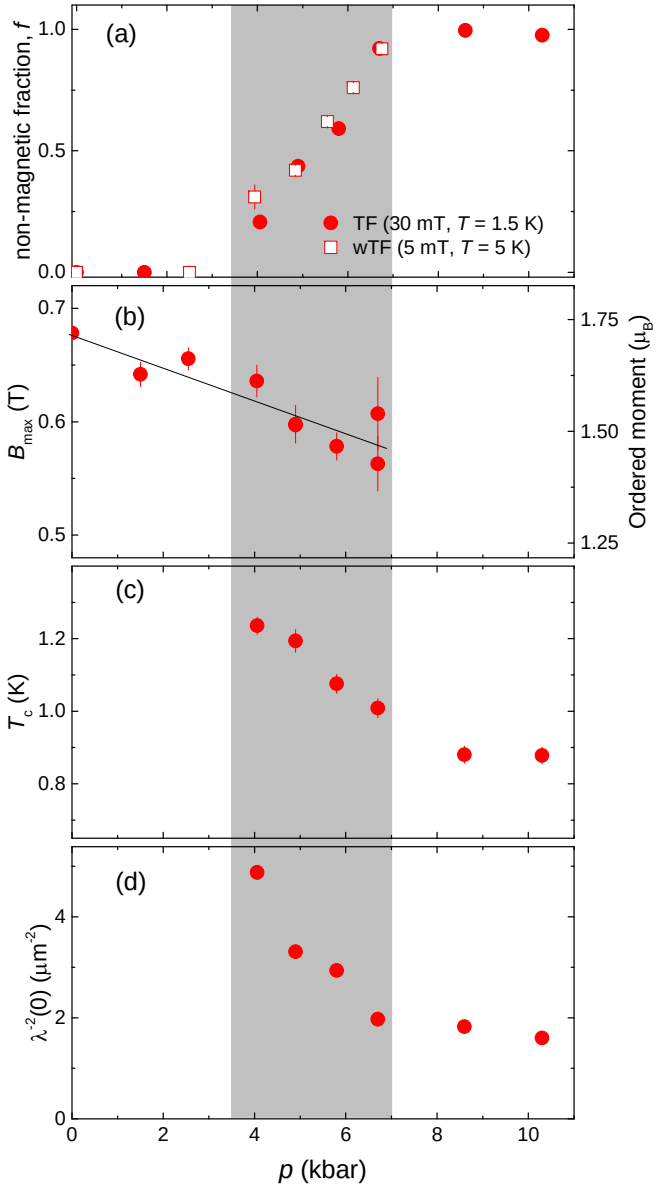

- Besides the competition for the volume, there is no evidence for a competition between the magnetic and superconducting order parameter in CrAs:
  1. The ordered magnetic moment stays almost constant, by changing less than 15%.
  2. T_N, evolves smoothly with pressure without showing any pronounced features at p~3.5-4kbar

- The maximum value of $\rho_s \sim \lambda^{-2} \sim n_s/m^*$ is observed at the low pressure side of the phase separated region -- in the region where the non-magnetic volume fraction *f* is the smallest.
- By neglecting the pressure effect on m*,

$$\rho_s \sim n_s$$

carriers from the 'less conductive' magnetically ordered parts of the sample can be supplied to the 'more conductive' non-magnetic parts -- self doping effect!

Conventional vs. unconventional superconductivity

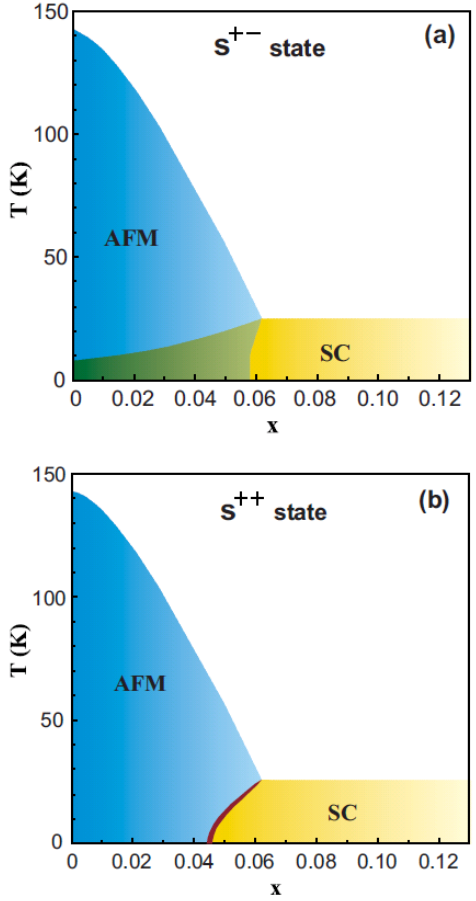

FIG. 1. (Color online) Phase diagrams of $Ba(Fe_{1-x}Co_x)_2As_2$ for a superconducting (a) s^{+-} state and an (b) s^{++} state, obtained by numerically solving the gap equations. The green region denotes homogeneous, microscopic coexistence, whereas the dark red region denotes heterogeneous, macroscopic coexistence. The band-structure parameters are discussed in Sec. IV B.

Fernandes et al., PRB 82, 014521 (2010)

- The relative phase difference (θ) of the superconducting order parameter between different parts of Fermi surface or Fermi surface sheets may lead either to stabilization of microscopic coexistence of the magnetic and superconducting phases or drive both to repel each others:

$$F_J \propto M^2|\Delta_1||\Delta_2|\cos\theta$$

– For conventional superconductivity $\Theta=0$, F_J increases making two phases unlikely to coexist

– For $\Theta=\pi$, F_J is negative. Both the superconducting and the magnetic phases tend to coexist.

Correlation between T_c and λ^{-2}

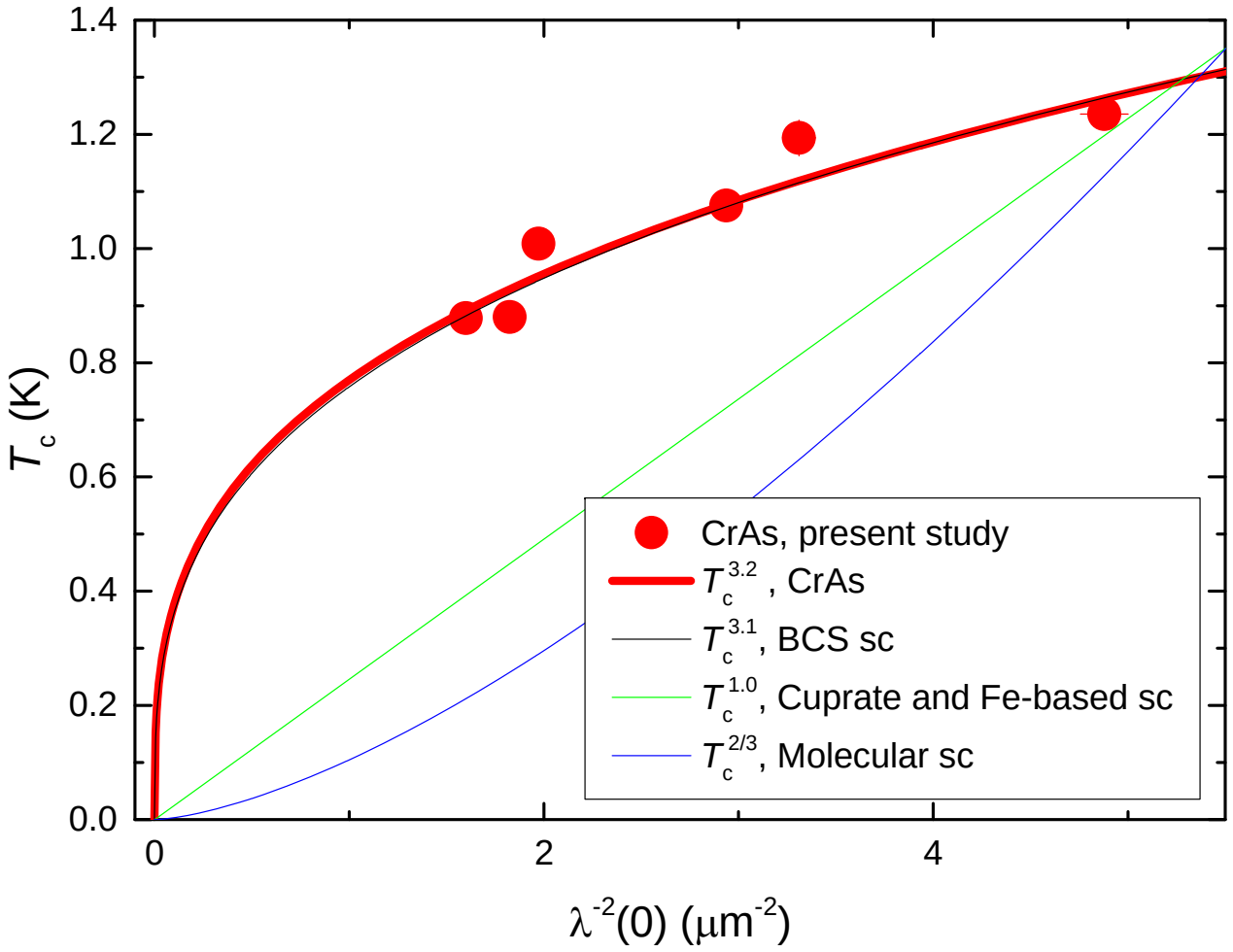

PAUL SCHERRER INSTITUT

Conclusions

- The bulk magnetism exists up to ***p***~3.5kbar, while the purely non-magnetic state develops for pressures above ~7kbar.
- In the intermediate pressure region (3.5<***p***<7kbar) the magnetic phase volume decreases continuously and superconductivity develops in parts of the sample remaining non-magnetic down to the lowest temperatures.
- Both, the superconducting transition temperature T_c and the zero-temperature superfluid density $\rho_s(0)$ decrease with increasing pressure in the intermediate pressure region and saturate for ***p*** exceeding 7kbar i.e. in the region where magnetism is completely suppressed.
- The pressure-induced transition of CrAs from a magnetic to a superconducting state is characterized by a separation in macroscopic size magnetic and superconducting volumes. The less conductive magnetic phase provides additional carriers (doping) to the superconducting parts of CrAs.
- The superfluid density was found to scale with T_c as $T_c^{3.2}$, which, together with the clear phase separation between magnetism and superconductivity, points towards a conventional mechanism of the Cooper-pairing in CrAs.

PAUL SCHERRER INSTITUT

Superfluid density and the symmetry of the superconducting gap

T-Dependence of the SC carrier density

From μSR:

$$\sigma_\mu = \gamma_\mu \sqrt{\langle \Delta B^2 \rangle} \quad \propto \quad \frac{1}{\lambda^2}$$

$$\lambda = \sqrt{\frac{m}{\mu_0 e^2 n_s}}$$

$$\Rightarrow \quad \sigma_\mu \propto \frac{\mu_0 e^2}{m} n_s$$

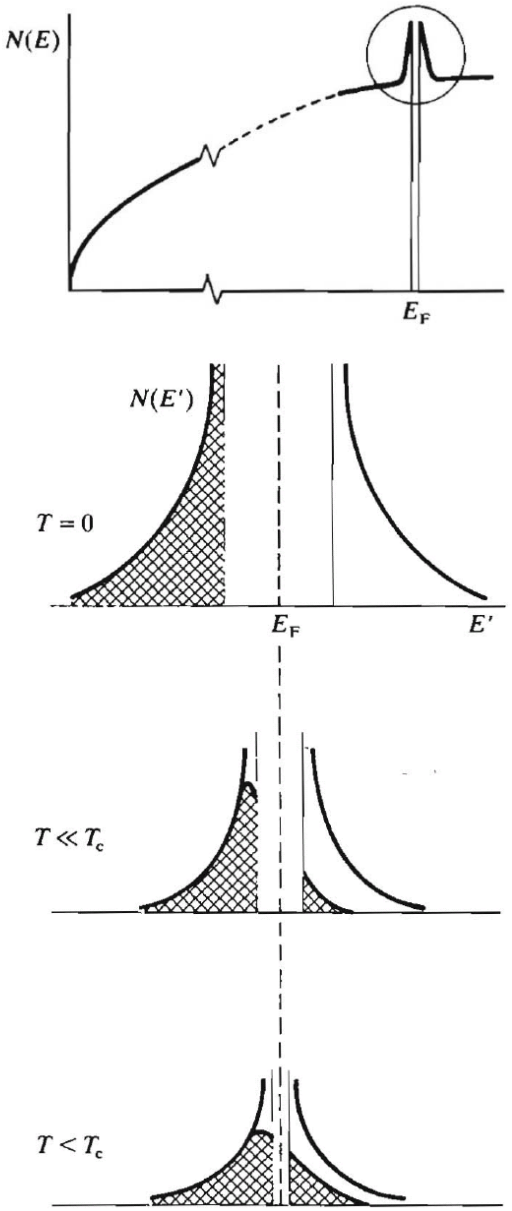

s-wave Superconducting Gap

- BCS conventional pairing: isotropic *s*-wave pairing

From μSR:

$$\sigma_\mu \propto \frac{1}{\lambda^2} = \frac{\mu_0 e^2}{m} n_S$$

$$n_S(T) = n_S(0)\left(1 - \frac{2}{k_B T}\int_0^\infty f(\varepsilon,T)[1-f(\varepsilon,T)]\,d\varepsilon\right)$$

and for an isotropic energy gap (s-wave):

$$n_S(T) = n_S(0)\left(1 - \sqrt{\frac{2\pi\Delta(0)}{k_B T}}\exp\left[-\frac{\Delta(0)}{k_B T}\right]\right)$$

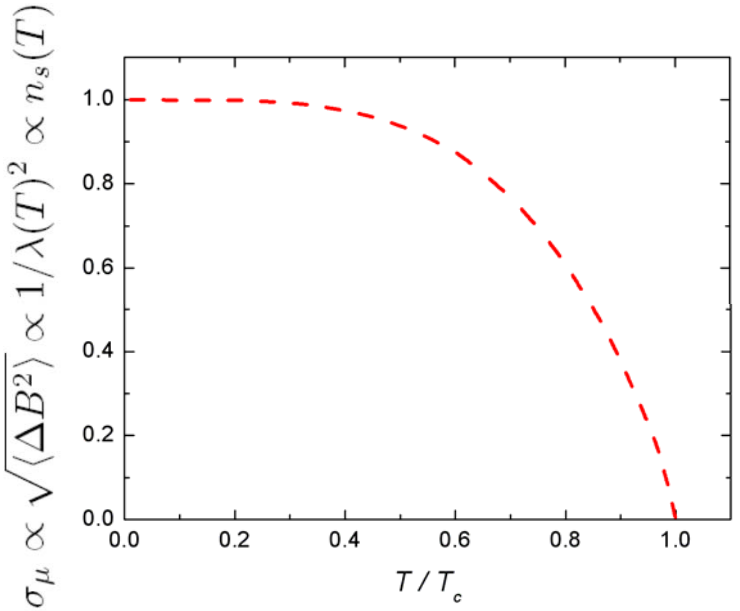

B. Mühlschlegel, Z. Phys. 155, 313 (1959)

s-wave Superconducting Gap – Examples

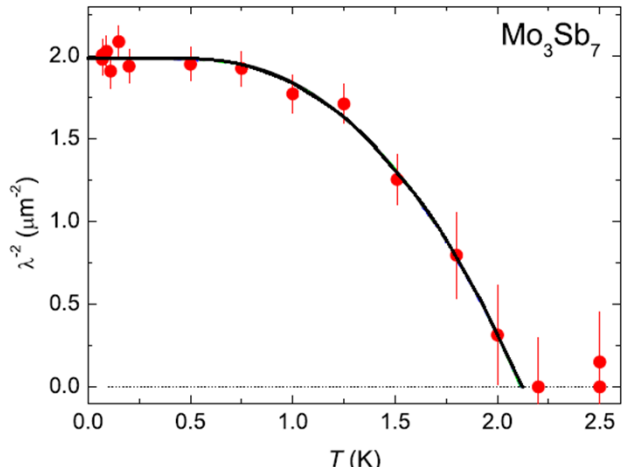

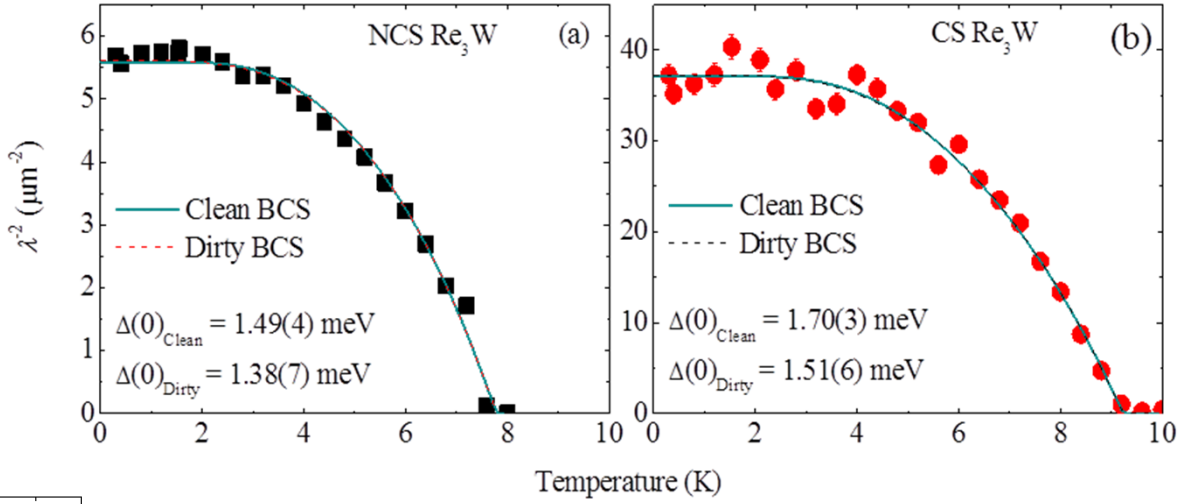

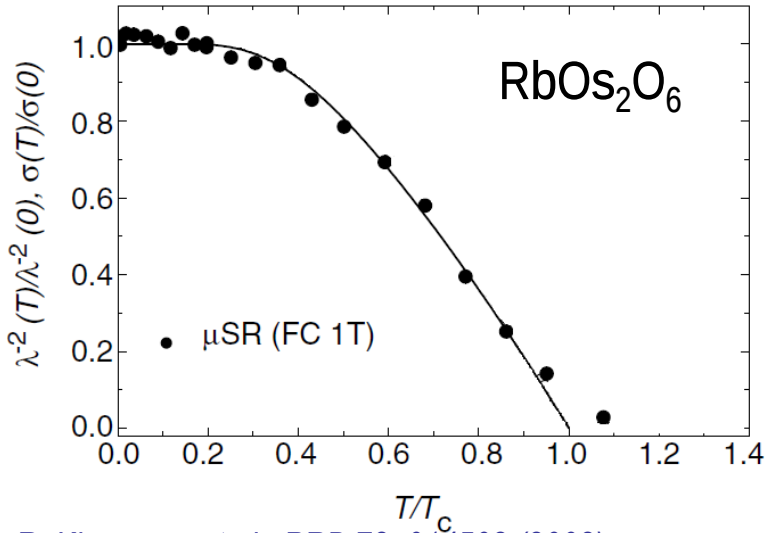

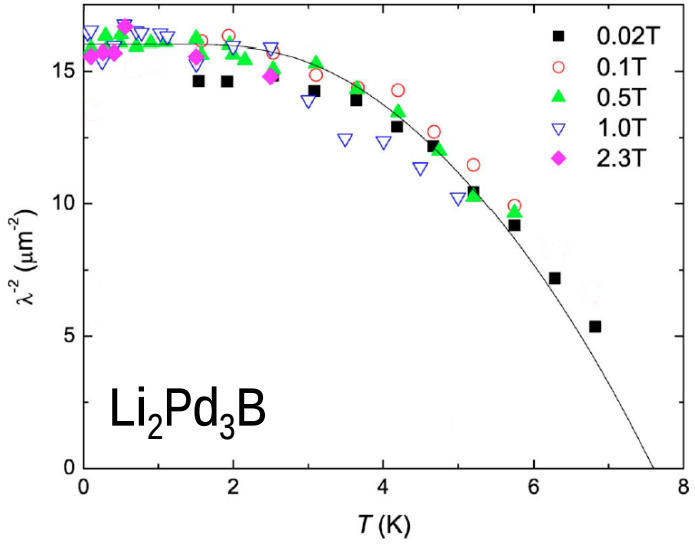

R. Khasanov et al., PRB 78, 014502 (2008)
P.K. Biswas et al., PRB 85, 134505 (2012)
R. Khasanov et al., PRB 72, 104504 (2005)
R. Khasanov et al., PRB 73, 214528 (2006)

Gap Symmetry in High-T_c's Cuprates

- ~~BCS conventional pairing: isotropic *s*-wave pairing~~

From μSR:

$$\sigma_\mu \propto \frac{1}{\lambda^2} = \frac{\mu_0 e^2}{m} n_S$$

$$n_S(T) = n_S(0)\left(1 - \frac{2}{k_B T}\int_0^\infty f(\varepsilon,T)[1-f(\varepsilon,T)]\,d\varepsilon\right)$$

and for an isotropic energy gap (s-wave):

$$n_S(T) = n_S(0)\left(1 - \sqrt{\frac{2\pi\Delta(0)}{k_B T}}\exp\left[-\frac{\Delta(0)}{k_B T}\right]\right)$$

B. Mühlschlegel, Z. Phys. 155, 313 (1959)

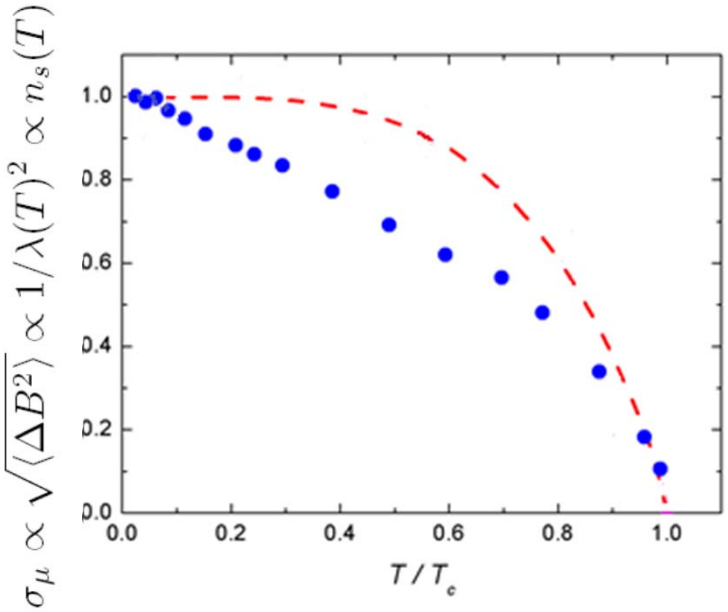

Single crystal $YBa_2Cu_3O_{6.95}$

*J.E. Sonier et al, PRL **72**, 744 (1994)*

Pairing Symmetry in High-Tc's Cuprates

s-wave SC state:

$$n_s(T) = n_s(0)\left(1 - \frac{2}{k_B T}\int_0^\infty f(\epsilon,T)\,[1-f(\epsilon,T)]\,d\epsilon\right)$$

with:

$$f(\epsilon,T) = \left(1+\exp\left[\sqrt{\epsilon^2+\Delta(T)^2}/k_BT\right]\right)^{-1}$$

d-wave SC state:

$$n_s(T) = n_s(0)\left(1 - \frac{1}{\pi k_B T}\int_0^{2\pi}\int_0^\infty f(\epsilon,T)\,[1-f(\epsilon,T)]\,d\varphi\,d\epsilon\right)$$

with:

$$f(\epsilon,T) = \left(1+\exp\left[\sqrt{\epsilon^2+[\Delta_s(T)\cos(2\varphi)]^2}/k_BT\right]\right)^{-1}$$

remembering that:

$$\lambda = \sqrt{\frac{m}{\mu_0 e^2 n_s}}$$

one gets: (for $T \ll T_c$)

$$n_s(T) \propto n_s(0)\left(1 - 2C\frac{T}{\Delta_s(0)}\right)$$

$$\lambda(T) \propto \lambda(0)\left(1 + C\frac{T}{\Delta_s(0)}\right)$$

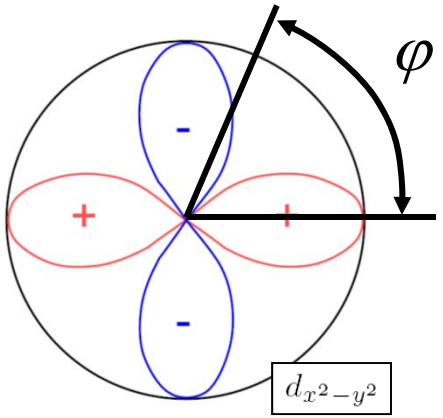

*Hirschfeld & Goldenfeld, PRB **48**, 4219 (1993)*

d-wave Superconducting Gap – Examples

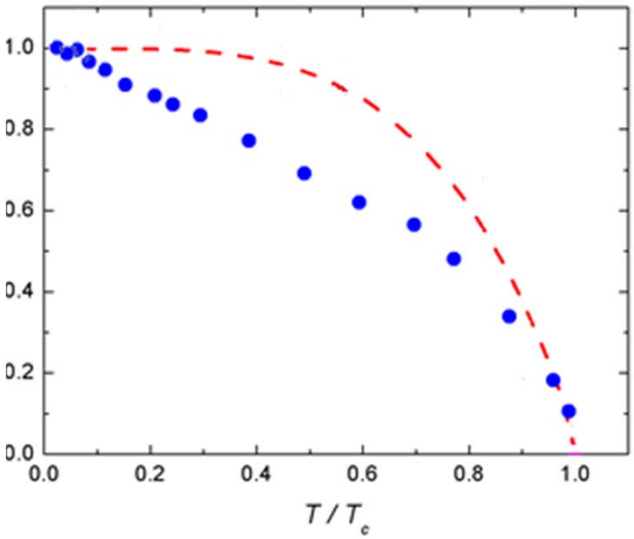

Single crystal $YBa_2Cu_3O_{6.95}$
*J.E. Sonier et al, PRL **72**, 744 (1994)*

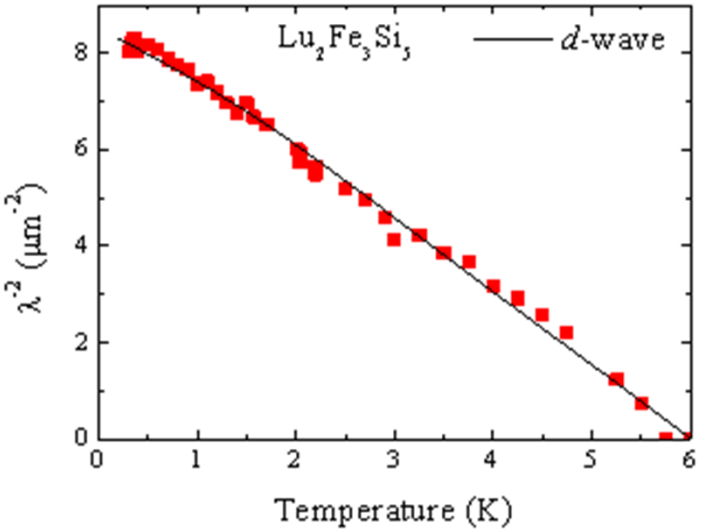

Single crystal $Lu_2Fe_3Si_5$
P. Biswas et al, in prep.(2014)

Multiband Superconductivity

ARPES on $Ba_{1-x}K_xFe_2As_2$:

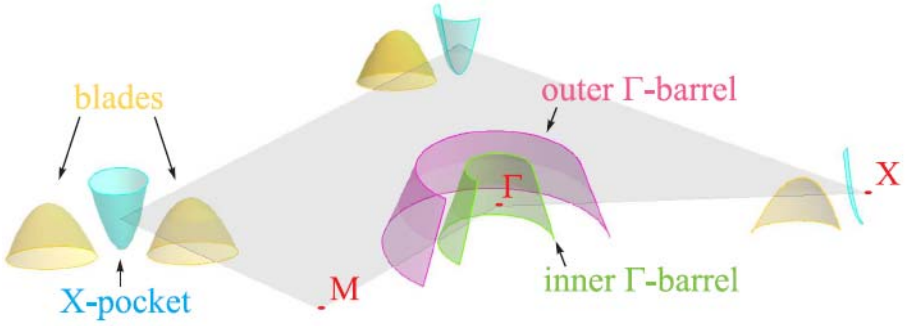

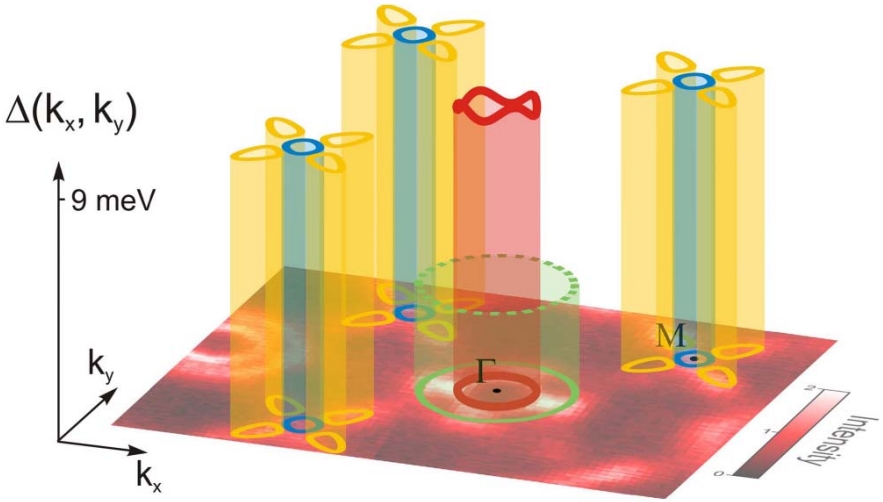

- Multiband superconductivity
- Nodeless gaps

$$\frac{\lambda^{-2}(T)}{\lambda^{-2}(0)} = \omega_1 \frac{\lambda^{-2}(T,\Delta_{0,1})}{\lambda^{-2}(0,\Delta_{0,1})} + \omega_2 \frac{\lambda^{-2}(T,\Delta_{0,2})}{\lambda^{-2}(0,\Delta_{0,2})}$$

V. B. Zabolotnyy *et al.*, Nature 457, 569 (2009).
D. V. Evtushinsky *et al.*,Phys. Rev. B 79, 054517 (2009).
D. V. Evtushinsky *et al.*, New J. Phys. 11, 055069 (2009).

Multiband Superconductivity – Examples

$Ba_{1-x}K_xFe_2As_2$

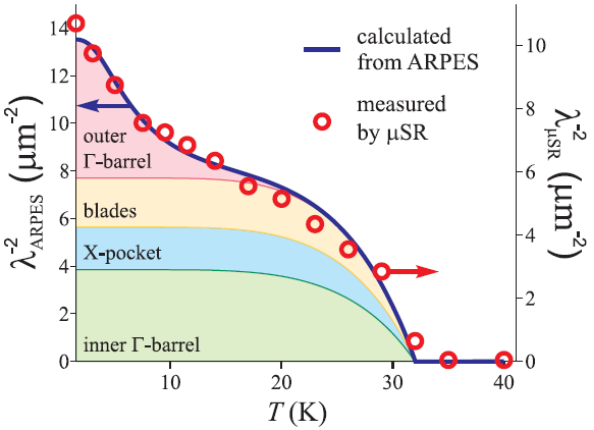

R. Khasanov *et al.*, PRL 102, 187005 (2009).

$FeSe_{1-x}Te_x$

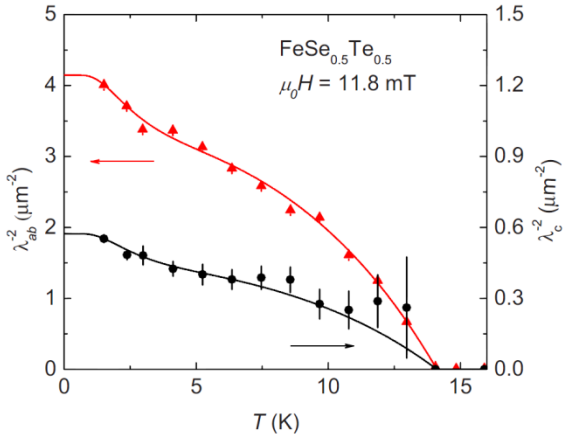

M. Bendele *et al.*, PRB 81, 224520 (2010).

$FeSe_{1-x}$

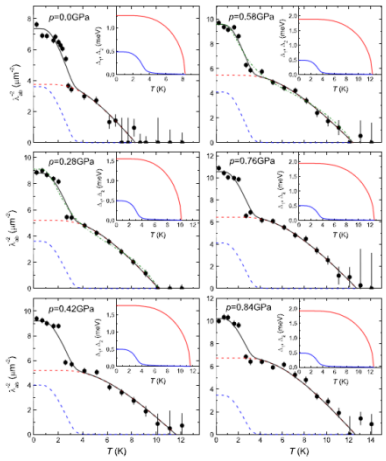

R. Khasanov *et al.*, PRL 104, 087004 (2010).

$RbFe_2As_2$

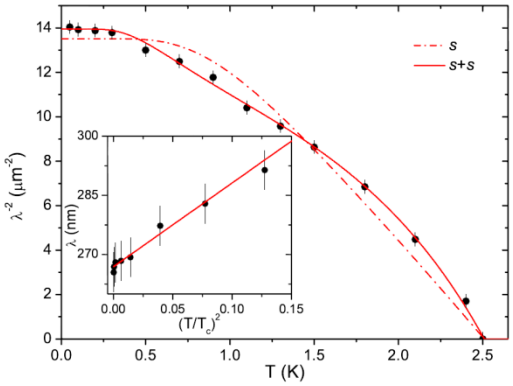

Z. Shermadini *et al.*, PRB 82 144527 (2010)

$BaFe_{2-x}Co_xAs_2$

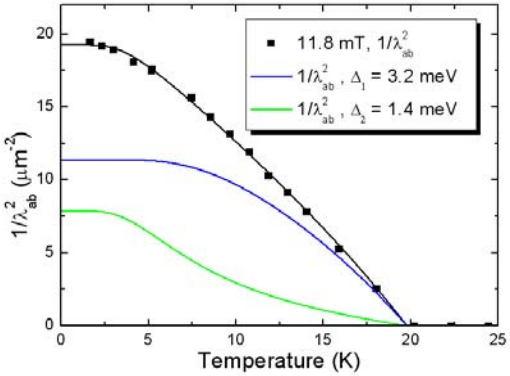

H. Luetkens *et al.*, in prep..

PAUL SCHERRER INSTITUT

Thank you for your attention!

Muon is a Local Magnetic Probe

Muon probes the local magnetism from within the unit cell

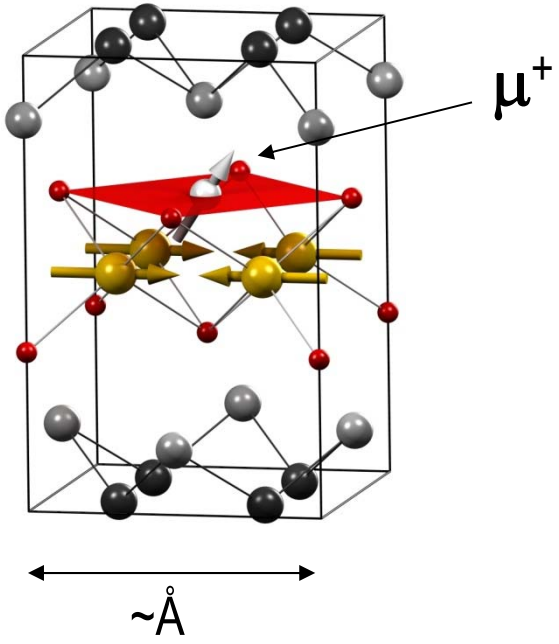

Muon probes the local magnetic response of a superconductor (Meissner screening or flux line lattice)

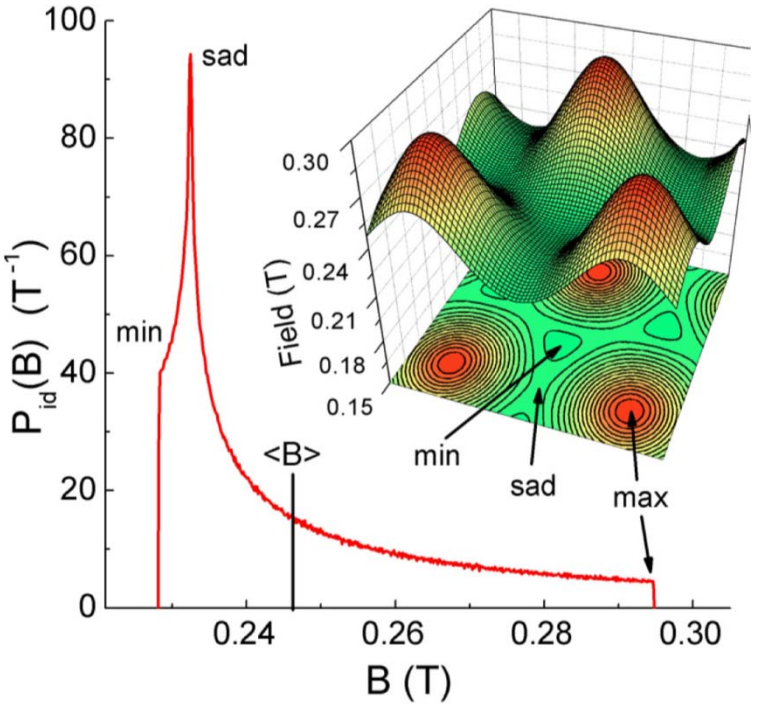

After H. Luetkens (Sunday 16 Aug 2015)